

Point-to-point response to reviewers' comments

The comments are in black, and our answers are in blue.

Reviewer #3:

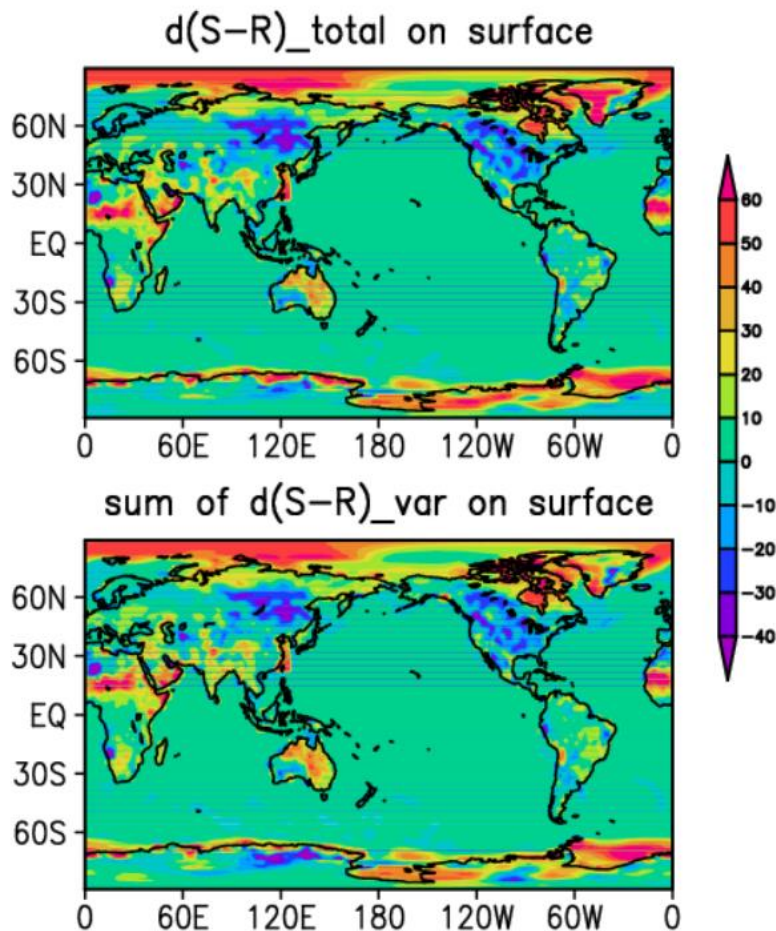
Zheng et al. examined the contribution of sea ice albedo effects and insulation effects on the Arctic amplification using EC-Earth climate model simulations of preindustrial and Pliocene forcing. The attribution of different effects is assessed by the climate feedback and response analysis method (CFRAM) and the equilibrium feedback assessment (EFA)-like approach. Their analysis showed that the ice albedo effects were related to the summer SST warming and the insulation effects were related to the surface air temperature warming in winter. The results of this study are important to the understanding of the Pliocene warming as well as to improve the projection for the present warming trend. The organization of this manuscript is clear and easy to follow. The clarity of presentation is one of my main concerns. Some confusion or ambiguity are likely due to language issues. I suggest the authors either carefully examine the manuscript for grammar issues sentence by sentence or consult a native speaker to improve the writing of the manuscript. The assumption of linearity is very important for the attribution assessment. The authors have not provided physical reasons to support this assumption. It would be useful to provide some uncertainty estimates due to the inherent limitation of the analysis methods. Therefore, I recommend a major revision to the manuscript before it can be accepted for publication.

We are grateful for the positive evaluation and detailed comments that follow.

- 1) We have corrected the grammar issues, a native English speaker has proofread the revised manuscript.
- 2) For the attribution assessment, CFRAM can linearly decompose radiative perturbation into individual contribution, including shortwave and longwave components, from CO₂, surface albedo, cloud, water vapour, and air temperature:

$$\Delta Q_{rad} = \Delta(S + R)_{co_2} + \Delta S_{albedo} + \Delta(S + R)_{cloud} + \Delta(S + R)_{wv} + \Delta R_T,$$

which can be validated by summing all the partial radiation perturbation from CFRAM output and comparing with the radiative perturbation output. They are almost identical (The figure is shown below), thus explaining the linearity.



Other main concern:

The experiment setup. (1) If the objective of this study is to understand the contribution of ice albedo effects and insulation effects on the Arctic warming, why is it necessary to use the Pliocene simulation in the current setup? In this case, there are lots of publicly available model output from CMIP3 and CMIP5 to provide more robust results. (2) As is stressed by the authors, the justification of performing the Pliocene warming simulation is the availability of the proxy data constraint from paleo-records. If the objective is to understand the Pliocene warming, however, the orbital forcing adopts preindustrial conditions. Does it make the justification of this Pliocene simulation irrelevant? The Pliocene is a long time period and authors have not stated clearly what period are simulated. Are the fixed CO₂ with PRISM surface conditions the default setting for the PlioMIP2 simulations? If so, please give a brief description of it and the justification for this choice. It will be very helpful for readers who are not familiar with the PlioMIP2.

(1) The Pliocene simulation is selected because of three reasons:

1) The Pliocene epoch, the most recent warm period with the similar CO₂ concentration as today, is an analogue of current or future climate change.

2) The Pliocene simulation can be partly verified by proxy data reconstructed from deep-sea oxygen isotope analysis, while the future projection from climate model is of high uncertainty owing to the lack of any validation.

3) Whereas the historical or undergoing climate variability is transient, the Pliocene simulation is obtained after the model integration reaches a quasi-equilibrium state. The equilibrium response is in principle reversible while transient response is hysteretic, suggesting that the Pliocene simulation can better represent a steady climate response.

(2) The Pliocene is a long time period, and mid-Pliocene Warm Period (3.264–3.025 Ma) is selected for Pliocene simulation in PlioMIP2, which has been stated clearly in the revised version. The orbital forcing adopts preindustrial conditions because mid-Pliocene Warm Period (3.264–3.025 Ma) has a near-modern orbital forcing. The CO₂ concentration 400ppmv is set in the Core PlioMIP2 experiment, and other details of the experiment, i.e., PRISM4 Pliocene palaeogeography reconstruction including topography, bathymetry, ice sheets and land–sea mask, etc., are proposed in PlioMIP2. A brief description is specified in Section 2.1 of the revised version.

Specific comments:

Line 14: Define PRISM.

The definition of PRISM is added.

Line 24: “CO2” to “CO₂”.

Done.

Line 24-25: This sentence seems to suggest the CO₂ increase is due to the monitoring. Please rephrase.

Changed to “As shown in the monitoring at ...”

Line 25-28: Break up this sentence to two sentences and rewrite.

Done.

Line 26: “increased 1.1°C to” change to “increased 1.1°C compared to”.

Done.

Line 31: “its reflectivity”. Do you mean the sea ice reflectivity changes is responsible to changes in surface energy budget, etc.? Please rephrase to clarify.

Both the sea ice reflectivity changes and the reduction in the insulating effect of sea ice are responsible to changes in surface energy budget. The sentence has been rephrased for clarity.

Line 47-54: Some justification for Pliocene simulation is provided here. But the simulation in this study use mixed Pliocene and preindustrial conditions. Can you still use proxy data to verify the simulation? Some comparison with proxy data are shown in Fig. 1 but performance constraint by proxy data is still qualitative.

The Pliocene simulation is set following the PlioMIP2 protocol. The orbital forcing adopts preindustrial conditions because mid-Pliocene Warm Period (3.264–3.025 Ma) is specified and has a near-modern orbital forcing. Referring to the review of Haywood et al. (2016) that “The temporal focus for PlioMIP2 has been matched to the data collection strategy adopted by PRISM4 to further enhance the connection between models and data and to improve the validity of future data/model comparisons.”, it is available to use proxy data (PRISM) to verify the simulation.

Line 146-147: It is not clear what “an approach” is referring to.
“an approach” has been specified.

Line 150: “linear”: do you have any reason to believe it should be linear. Please provide some argument to support this assumption or reference previous studies to support your statement.

The heat flux depends not only on sea ice, but also on other variables, e.g., wind speed. In addition to considering the interaction at the interface, the heat flux is not strictly linear with sea ice. Therefore “linearity” assumed here is to investigate the linear impact of sea ice on the heat flux. The following correlation analysis can be used to evaluate to what extent it can be linear, e.g., the high correlation coefficient between shortwave radiation change due to albedo and sea ice concentration change indicates the albedo effect of sea ice on shortwave radiation is nearly linear.

Line 162: The choice of student-t test assumes Gaussian distribution. However, it is usually not the case for geophysical parameters. The spatial and temporal autocorrelation are not taken into account. The bootstrap method adopted by Liu et al. (2012) is more relevant, especially when “moving-block” is used to represent the length scale of the spatial or temporal features (van de Poll et al., 2006; Z. Liu et al., 2010).

The spatial correlation and student-t test applied in the study are based on the effective number of spatial degrees of freedom (Bretherton et al., 1999), in which non-normally distributed data could be estimated and the spatial autocorrelation was

taken into account. Moreover, Bretherton et al. (1999) also found close agreement between the actual PDF and a fitted distribution based on Monte Carlo simulation with the effective number of spatial degrees of freedom.

Line 174-179: It is not clear what message these sentences are trying to convey. Is the Arctic amplification stronger in Pliocene simulation or not?

These sentences are written to introduce the Arctic amplification in Pliocene based on proxy data, as well as some explanations for the stronger Arctic amplification in Pliocene. Yes, the Arctic amplification is stronger in Pliocene simulation.

Line 180: Not exactly the SST and SAT in “Pliocene epoch”. They are from the Pliocene simulations using some of the Pliocene conditions.

The Pliocene simulation is a Core PlioMIP2 experiment, and the temporal focus for PlioMIP2 is the mid-Pliocene warm period, so “Pliocene epoch” is changed to “the mid-Pliocene warm period”.

Fig. 1: The overlay of proxy data over the filled contour maps does not show the difference well. An additional map showing the differences might be more informative. Maybe add it to supplement?

Thanks for your suggestion. The difference of annual mean SST anomaly (Pliocene minus preindustrial) between EC-Earth simulation and the proxy data is shown in Figure S2. The underestimation in high latitude regions, similar to multi-model mean in Dowsett et al. (2012) but significantly less in bias.

Line 187: “off America”. Do you mean USA or the America continents? The coastal warming is not very obvious or extensive in either. The warming off the west coast of Africa is more obvious. By “permanent El Nino-like feature”, I expect to see extensive warming in equatorial eastern Pacific, which is not present in Fig. 1. Am I missing anything?

The comment is no longer applicable as the description of the tropical anomalies has been removed because the paper’s focus is on the Arctic response (as suggested by Reviewer #4).

Line 197: “very sensitive” to what? “preindustrial” is used noun here and in several other occasions. Please add proper noun after it so that it is clear what it is referring to.

Referring to the comment of Reviewer #4 (“The first line of this paragraph contains little meaning”), we have removed the sentence, thus “very sensitive” is no longer applicable. A proper noun is added after “preindustrial” throughout the paper.

Line 200-201: Please rephrase this sentence.

The sentence has been rewritten.

Line 201: The definition of heat loss or heat gain is not given here. Consider move up the definition in line 204-208 before they are discussed.

The definition of heat loss or heat gain has been moved up as suggested.

Fig. 5: What are these dots? Are they differences between corresponding years in Pliocene and preindustrial runs? Does it matter how you pair up the years in Pliocene and preindustrial runs? Would it change the response coefficients? How much uncertainty would it introduce?

In this study the last 100-year-mean of all variables are used for analysis, and the Pliocene climate anomalies are calculated by subtracting the mean of the preindustrial simulation without trends removal. Thus each dot in this figure represents one grid point value of the Pliocene sea ice concentration anomaly and shortwave anomaly due to albedo over the Arctic Ocean, which is specified in the revised version for clarity. They are not the differences between corresponding years in Pliocene and preindustrial runs, and it doesn't matter how you pair up the years in Pliocene and preindustrial runs. The response coefficients depend on the linear regression coefficient of these dots. The uncertainty can be expressed as a confidence interval, i.e., 1.96 standard errors either side of the estimate.

Line 242: How do you define “anomalies”? Are they with respect to the 100-year Arctic averages, Arctic monthly mean, or something else? Please describe clearly. Otherwise, it is impossible to interpret Table 1 to Table 4.

The “anomalies” are defined in Section 2. (In this study the last 100-year-mean of all variables are used for analysis, and the Pliocene climate anomalies are calculated by subtracting the mean of the preindustrial simulation without trends removal.) Thus here they are with respect to Arctic monthly mean while discussing seasonal variation, and this is specified in the revised version.

Line 252-253: This sentence is confusing. Please rewrite.

The sentence is rewritten.

Line 263: Again, do you have any reason to believe they should be linear?

As mentioned above, the heat flux depends not only on sea ice, but also on other variables. In addition to considering the interaction at the interface, the heat flux is not strictly linear with sea ice. Therefore “linearity” assumed here is to investigate the

linear impact of sea ice on the heat flux. The following correlation analysis can be used to evaluate to what extent it can be linear, e.g., the high correlation coefficient between shortwave radiation change due to albedo and sea ice concentration change indicates the albedo effect of sea ice on shortwave radiation is nearly linear.

Line 274: What do you mean by “significant interaction”?

The phrase “significant interaction” is unclear and is changed to “linear relationship”.

Line 276-284: The partition of ice-free and ice-covered conditions is confusing. How do you have SIC changes when it is ice-free?

The partition threshold of ice-free and ice-covered conditions is 15% sea ice concentration as commonly used in sea ice study, which is specified in the revised version. The “ice-free” shown in Figure 9 represents that the sea ice of the grid points varies from the preindustrial ice-covered status to the Pliocene ice-free status, so SIC change can be calculated as the SIC difference between the Pliocene and the preindustrial period.

Fig. 9: Is the regression line with respect to the ice-covered only? Would the regression line be different between ice-covered and ice-free? You would expect so because it is why you separate them in the first place.

Yes, the regression line is with respect to the ice-covered only, and it is specified in the figure caption. It can be inferred from Figure 9 that the regression line is different between ice-covered and ice-free conditions.

Line 289-293: I am confused with the definition of ice-free and ice-covered changes relative to SIC. So I cannot follow the argument here. I will have to revisit after the authors’ clarification.

The paragraph intends to explain the linear regressions of sensible and latent heat flux anomalies on SIC, including slope and intercept. As mentioned above, the ice-free (ice-covered) shown in Figure 9 represents that the sea ice of the grid points varies from the preindustrial ice-covered status to the Pliocene ice-free (ice-covered) status.

Line 297-299: Does the melting of sea ice refer to the sea ice melt in spring or due to warming by high CO₂? Are you sure it is conduction not convection?

The melting of sea ice refers to the sea ice melts due to warming by high CO₂, which is specified in the revised version.

We think that conduction moves the heat from sea/ice to the atmosphere at the surface and then convection moves the heat upward to higher level of atmosphere.

References:

- Liu, Y., Key, J. R., Liu, Z., Wang, X., & Vavrus, S. J. (2012). A cloudier Arctic expected with diminishing sea ice. *Geophysical Research Letters*, 39(5).
<https://doi.org/10.1029/2012GL051251>
- Liu, Z., Marchand, R., & Ackerman, T. (2010). A comparison of observations in the tropical western Pacific from ground-based and satellite millimeter-wavelength cloud radars. *Journal of Geophysical Research: Atmospheres*, 115(D24), D24206.
<https://doi.org/10.1029/2009JD013575>
- van de Poll, H. M., Grubb, H., & Astin, I. (2006). Sampling uncertainty properties of cloud fraction estimates from random transect observations. *Journal of Geophysical Research: Atmospheres*, 111(D22), D22218. <https://doi.org/10.1029/2006JD007189>

Contribution of sea -ice albedo and insulation effects to Arctic amplification in the EC-Earth Pliocene simulation

Jianqiu Zheng^{1,2,3}, Qiong Zhang¹, Qiang Li¹, Qiang Zhang¹, Ming Cai⁴

¹Department of Physical Geography and Bolin Centre for Climate Research, Stockholm University, Stockholm, 10691, Sweden

²School of Earth and Space Sciences, University of Science and Technology of China, Hefei, 230026, China

³Key Laboratory of Meteorological Disaster of Ministry of Education, Nanjing University of Information Science and Technology, Nanjing, 210044, China

⁴Department of Earth, Ocean and Atmospheric Science, Florida State University, Tallahassee, Florida, 32306, USA

Correspondence to: Jianqiu Zheng (qiu@ustc.edu.cn)

Abstract. In the present work, we simulate the Pliocene climate with the EC-Earth climate model as an analogue equilibrium state for current warming climate induced by rising CO₂ in the atmosphere. The simulated Pliocene climate shows a strong Arctic amplification featured by featuring pronounced warming sea surface temperature (SST) over the North Atlantic, in particular over Greenland Sea and Baffin Bays, which is comparable with geological SST reconstructions from the Pliocene Research, Interpretation and Synoptic Mapping group (PRISM-, Dowsett et al., 2016). To understand the underlying physical processes, the air-sea heat flux variation in response to Arctic sea -ice change is quantitatively assessed by a climate feedback and response analysis method (CFRAM) and an approach similar to equilibrium feedback assessment -(EFA)-like approach- Giving. Given the facts fact that the maximum SST warming in-SST occurs in summer while the maximum warming in surface air temperature warming happens during winter, our analyses show that a dominant ice-albedo effect is the main reason for summer SST warming, and a 1% loss in sea -ice concentration could lead to an approximate 21.8 Wm⁻² increase in shortwave solar radiation into open sea surface. During winter month months, the insulation effect induces enhanced turbulent heat flux out of the sea surface due to sea -ice melting in previous summer months. This leads to more heat releaser released from the ocean to atmosphere, thus explaining the-stronger why surface air temperature warming amplification is stronger in winter than in summer.

1 Introduction

Through As shown in the monitoring at Mauna Loa Observatory in Hawaii (<https://www.esrl.noaa.gov/gmd/obop/mlo/>), the CO₂ concentration in the atmosphere had-steadily passed the 400 ppm threshold by September 2016. Accordingly, global mean temperature in 2016 increased by about 1.1 °C compared to that-of the preindustrial period, as released by the World Meteorological Organization (<https://public.wmo.int/en/media/press-release>), —one). One major consequence of this continuing and accelerating warming is the rapid melting of ice in at high latitudes. Ten The ten lowest minimum Arctic sea -ice extents since satellite records were made available in 1979 have taken place in recent happened in every year of the last

decade except for 2005, as documented by National Snow and Ice Data Centre. Moreover, ~~an~~ ice-free Arctic Ocean is estimated to emerge ~~in~~ around 2050 on the basis of climate model projections (Overland et al., 2011). As ~~the~~ sea -ice retreats, ~~its reflectivity~~ the surface of the Arctic Ocean becomes less reflective and ~~insulation decrease~~ the enhanced open-ocean region leads to greater air-sea heat exchange due to the reduced insulating effect of sea ice. This leads to ~~the~~ changes in the surface heat budget, and ~~the~~ changes in overlying cloud and water vapour, further ~~amplify the~~ amplifying Arctic warming and sea -ice melting. Many studies have shown that the accelerated Arctic sea -ice retreat ~~is~~ possibly ~~resulted~~ results from local ice-albedo positive feedback (Winton, 2008), meridional heat transport by atmospheric circulation and oceanic current (Alexeev et al., 2013), or sea -ice drift out of the Fram Strait (Nghiem et al., 2007; Krumpen et al., 2016). In turn, Arctic sea -ice decline can result in a variety of impacts on climate change, such as Arctic amplification (Serreze et al., 2009), change of cloud cover and precipitation (Liu et al., 2012; Bintanja and Selten, 2014), shift in atmospheric circulation pattern (Alexander et al., 2004), and slow-down of the Atlantic Meridional Overturning Circulation (Sévellec et al., 2017). A detailed consequence of Arctic sea -ice decline classified by local and remote effects ~~have~~ has been reviewed by Vihma et al. (2014).

Such ongoing high CO₂ level and low ice concentration in the Arctic is not unique in Earth's history. Geological data show that during the Pliocene, the CO₂ concentration in the atmosphere ~~did reach~~ reached 400 ppm or even more, and extreme warmth and Arctic amplification are recorded in multi-proxy evidence, including the longest and most complete record from Lake El'gygytyn, an undisturbed Siberian lake in northeast Arctic Russia (Brigham-Grette et al., 2013). Seasonally ice-free conditions existed in some Arctic regions in the mid-Pliocene until ~~the~~ circulation through the Bering Strait reversed ~~and, at which point~~ the excess freshwater supply might have facilitated sea -ice formation (Matthiessen et al., 2009). Several climate models have simulated the Pliocene but failed to reproduce the strong Arctic amplification ~~showed~~ shown in geological proxy data (Dowsett et al., 2012). While most of the previous studies on ~~contribution~~ the contributions of the sea -ice effect to Arctic amplification focus on contemporary ~~trend~~ trends or future ~~projection~~ projections, here the Pliocene simulation is selected ~~because of~~ for three reasons: (1) The Pliocene epoch (~~~~~ approximately 3 million years ago), the most recent warm period with ~~the CO₂ concentrations~~ similar ~~CO₂ concentration~~ as today, is not only an analogue of future climate change but also an appropriate past time-slice to examine regarding sea -ice effect (Haywood et al., 2016a). (2) The Pliocene simulation can be partly verified by proxy data reconstructed from deep-sea oxygen isotope analysis (Dowsett et al., 2012), while projecting the future ~~projection~~ from a climate model is of high uncertainty owing to the lack of any validation. (3) Whereas the historical or undergoing climate variability is transient, the Pliocene simulation is obtained after the model integration reaches ~~a~~ quasi-equilibrium-state. As inferred from Li et al. (2013), the equilibrium response is in principle reversible, while transient response is hysteretic, suggesting that the Pliocene simulation can better represent a steady climate response.

Two physical ~~attributions~~ characteristics of sea -ice are considered to affect climate system. One is much higher surface reflectivity of ice than that of open water, and the other is that ice can inhibit or reduce the exchange of momentum, heat, and mass between the atmosphere and ocean, ~~hereafter~~. Hereafter we refer these two ~~attribution~~ effects as “albedo” and

“insulation-effects,” respectively. Most previous studies on the two effects are mainly carried out by sensitivity experiments with the atmospheric general circulation model (AGCM). For instance, Gildor et al. (2014) examined the role of sea-ice ~~on~~in the hydrological cycle using the Community Atmospheric General Circulation Model (CAM3). ~~Two~~The two effects are separated by modifying the sea-ice albedo to that of open-water, or setting the sea-ice thickness to zero ~~but its albedo and~~ keeping albedo unchanged. Their results show that the insulation effect on the hydrological cycle is larger than the albedo effect, and these two effects are not independent, i.e. their total effect is not the sum of their separate contribution. Lang et al. (2017) also pointed out that the sea-ice thinning in recent years can lead to a 37% increase ~~37%~~ of Arctic amplification through the enhanced insulation effect, as estimated by an AGCM. Note that sea surface temperature (SST) is prescribed in their AGCM simulation, while sea-ice albedo or thickness is modified. In fact, the modification of sea-ice does not closely match the fixed SST ~~closely~~, which may lead to a bias in the sea-ice effect estimation from the AGCM simulation. The climate system, in turn, reinforces sea-ice loss while influenced by albedo or insulation ~~effect~~effects, which ~~is~~are known as ice-albedo feedback or ice-insulation feedback. In addition, albedo ~~effect~~ and insulation ~~effect~~ ~~interacts~~interact in a nonlinear way (Gildor et al., 2014). These feedbacks and ~~interaction~~interactions add more challenges to ~~understand~~understanding the effect of sea-ice on climate. Recently, Burt et al. (2016) and Kim et al. (2016) addressed the relationship between sea-ice loss and air-sea interface heat budget using the Community Earth System Model (CESM) simulation and cyclo-stationary empirical orthogonal function (CSEOF) analysis, respectively. However, the studies contain large uncertainties due to the hysteresis of transient processes (Li et al., 2013). Although the surface heat budget is the most fundamental ~~to aspect of~~ air-sea interaction, it is still not clear to what ~~degree~~extent heat flux responds to the change of Arctic sea-ice. Therefore the present study aims to quantitatively assess the variation of each individual component of air-sea heat flux caused by the decrease of Arctic sea-ice albedo and insulation. The analysis is based on the EC-Earth simulation of the Pliocene climate, which ~~representing~~represents an analogue for a future climate at equilibrium ~~climate~~with modern greenhouse gas levels, and the reference state is preindustrial equilibrium climate state.

The remainder of the paper is organized as follows. Section 2 describes the EC-Earth model and experimental design, and introduces the climate feedback and response analysis method (CFRAM) ~~),~~ as well as the approach to extract the impact ~~contributed from~~ of sea-ice loss. In ~~section~~Section 3, we present several climate features simulated in the Pliocene experiment. The albedo and insulation effects of sea-ice on air-sea interface heat flux are investigated in Sections 4 and 5, respectively ~~in sections 4 and 5,~~ followed by summary and discussion in ~~section~~Section 6.

2 Model and method

2.1 Model description and experimental design

The model applied in the study is the global coupled climate model EC-Earth (version 3.1, Hazeleger et al., 2012). Its atmospheric component is the Integrated Forecast System (IFS, version cycle 36r4) developed at the European Centre for Medium-Range Weather Forecast (ECMWF), including the land model H-TESSEL (Balsamo et al., 2009). This atmospheric

spectral model is run at T159 resolution (roughly 1.125°, ~~~approximately~~ 125 km) with 62 vertical levels and coupled to ~~thean~~ ocean component ~~that is~~ based on the Nucleus for European Modelling of the Ocean (NEMO, version 3.3, Madec, 2008) and the Louvain-la-Neuve sea-ice Model (LIM, version 3, Vancoppenolle et al. 2009). ~~The~~ NEMO ~~iswas~~ developed at the Institute Pierre Simon Laplace (IPSL) and has a resolution of about 1° and 46 vertical levels. In LIM3, surface albedo parameterization follows Shine and Henderson-Sellers (1985) with the following values: thick dry snow 0.8, thick melting snow 0.65, thick frozen bare ice 0.72, thick melting bare ice 0.53, and thin melting ice 0.47. The tuning of bare ice and snow albedo would affect whether the equilibrium ice thickness is reasonable and whether the ice is from a multi-year or seasonal ice zone. The coupling between the atmosphere and ocean/sea-ice is through the Ocean Atmosphere Sea-ice Soil coupler (OASIS, version 3.0, Valcke, 2006). EC-Earth has been used to examine the Arctic climate for the historical period and future scenarios in CMIP5. An evaluation of EC-Earth for the Arctic shows that the model simulates the 20th century Arctic climate reasonably well. EC-Earth simulated cloud variables with slightly larger cloud fraction and less cloud condensate ~~compared tothan~~ ERA-Interim, which ~~leadled~~ to similar longwave cloud radiative forcing. Moreover, total cloud forcing in EC-Earth is in good agreement ~~toewith~~ the APP-x satellite estimates (Koenigk et al., 2013). Koenigk et al. (2013) showed that the annual mean surface temperature in the Arctic increases by 12 K in the EC-Earth RCP8.5 scenario simulation, and the most pronounced warming is during autumn and winter in the lower atmosphere. A likely ice-free Arctic is indicated in September around 2040. The enhanced oceanic meridional heat flux into the Arctic (Koenigk et al., 2013) and the enhanced atmospheric northward latent energy transport (Graversen and Burtu, 2016) are suggested as major contributors to ~~the~~ future Arctic warming in the EC-Earth simulation. ~~Recently the~~ The EC-Earth model ~~ishas~~ also been applied to understand ~~the~~ past ~~elimateclimates~~, such as changes in the ~~change-of~~ Arctic climate (Muschitiello et al., 2015), African ~~monsoonmonsoons~~ (Pausata et al., 2016; Gaetani et al., 2017), tropical ~~eyelonecyclones~~ (Pausata et al., 2017a)), and ENSO activity (Pausata et al., 2017b) during the mid-Holocene. In this study we apply the model to the mid-Pliocene climate and focus on the effects of sea-ice on Arctic climate change.

Two numerical experiments are performed with EC-Earth to facilitate this study. One is the preindustrial control run with the 1850 CO₂ concentration of 284.725 ppm, and the other is the mid-Pliocene warm period (3.264–3.025 Ma) sensitivity experiment in which the atmospheric CO₂ concentration is set to 400 ppm. Following the protocol of the Pliocene Model Intercomparison Project, phase 2 (PlioMIP2, Haywood et al., 2016b), several configurations are modified in the Pliocene simulation: (1) in the Pliocene experiment, all ~~other~~ trace gases ~~exceptother than~~ CO₂, such as CH₄ ~~and~~ N₂O, and aerosols ~~in the Pliocene experiment~~, are specified ~~to-beas~~ identical to the preindustrial run to account for the absence of proxy data. (2) Orbit forcing, including eccentricity, obliquity, and precession, remains same within the preindustrial run as in the mid-Pliocene warm period, which has a near-modern orbital forcing. (3) Enhanced boundary ~~conditionconditions~~ from the Pliocene Research, Interpretation and Synoptic Mapping group (PRISM, Dowsett et al., 2016)), including land-sea mask, topography, bathymetry, and ice-sheet, are applied in the Pliocene experiment ~~where the land-sea mask, orography, bathymetry, vegetation~~. The global distributions of lake, soil, and ice-sheetbiome are modified accordingly to match the new land-sea mask and ice reconstruction. The integrations of the preindustrial control run and the Pliocene experiment are

carried out for 500 years, and it takes ~~approximate~~approximately 300 years for ~~the~~ model to reach equilibrium. From our last 200 years ~~of~~ output in the Pliocene simulation (see Figure S1 in the Supplement), the mean top of the atmosphere (TOA) net radiation is about -0.5 Wm^{-2} and its trend is near zero. The trend of mean SST is about 0.027 K/century, which fulfils the PMIP4 criterion that the trend of mean SST should be less than 0.05 K/century (Kageyama et al., 2018). In this study, the last 100-year-mean of all variables are used for analysis, and the Pliocene climate anomalies are calculated ~~with respect to by subtracting the mean of the preindustrial control run. The Arctic insimulation without trends removal.~~ In the following analysis, the Arctic is defined as the region poleward of 70 °N.

2.2 Climate feedback and response analysis method (CFRAM)

~~Radiative forcing varies as CO₂ concentration increases~~Climate system warming in the Pliocene experiment is driven by variation in radiative forcing, which ~~drives climate system warming is in turn caused by increased CO₂ concentration.~~ In response to temperature change, factors such as surface albedo, cloud, water vapour, and air temperature will adjust and feedback until the climate system reaches equilibrium. The contribution from each factor can be quantitatively evaluated by climate feedback analysis. ~~The traditional~~Traditional climate feedback analysis ~~method~~methods, such as partial radiative perturbation ~~(PRP) technique~~, is based on TOA radiative budget (Wetherald and Manabe, 1988), while the radiative kernel method can be extended to the surface and remain computationally efficient (Soden and Held, 2006; Pithan and Mauritsen, 2014). However, none of them takes individual physical processes into account, particularly non-radiative processes. ~~The climate feedback and response analysis method (CFRAM),~~ proposed by Lu and Cai (2009), overcomes this limitation.

CFRAM contains two parts: one is decomposing radiative perturbation into individual contribution, including shortwave and longwave components, from CO₂, surface albedo, cloud, water vapour, and air temperature. ~~It:~~

$$\Delta Q_{rad} = \Delta(S + R)_{CO_2} + \Delta S_{albedo} + \Delta(S + R)_{cloud} + \Delta(S + R)_{WV} + \Delta R_T, \quad (1)$$

where ΔQ_{rad} is performed by offline calculation using total radiative transfer model (Fu and Liou, 1993) with flux perturbation at the output from surface (ice and ocean), ΔS and ΔR are the preindustrial control run and net shortwave and longwave radiative perturbations at the Pliocene sensitivity experiment surface, respectively, and the subscripts CO₂, albedo, cloud, WV, and T represent the partial radiative perturbation due to changes in the CO₂ concentration, surface albedo, cloud properties, atmospheric water vapour, and air temperature, respectively. Note that here it is assumed that the interactions among the factors (CO₂, surface albedo, cloud, water vapour, and air temperature) are negligible and the higher order terms of each factors are omitted. The other part is calculating partial ~~temperatetemperature~~ perturbation due to individual radiative and non-radiative feedback processes, which is based on total energy balance and derived from the relationship between longwave radiation and temperature change. A more detailed description about CFRAM can be found in Lu and Cai (2009).

CFRAM is a practical diagnostic tool to ~~analyze~~analyse the role of various forcing and feedback agents and has been used widely in climate change research (e.g. Taylor et al., 2013; Song and Zhang, 2014; Hu et al., 2017). In the present study,

total radiative flux perturbation is first calculated from the surface radiative flux difference between the Pliocene sensitivity experiment and the preindustrial control run. Then we apply the first part of CFRAM to ~~obtain the surface radiative flux~~ compute each partial radiative perturbation, which is performed by offline calculation using a radiative transfer model (Fu and Liou, 1993). The linear approximation in Equation (1) should be verified with the output from the radiative transfer model. Finally, the partial radiative perturbation due to albedo, cloud, and water vapour, ~~and link it can be used~~ to evaluate albedo or insulation ~~effeteffects~~ of sea -ice.

2.3 Approach to extract sea -ice effects

As sea -ice declines in the Pliocene warming climate, ~~air-sea~~ heat flux ~~at air-sea interface~~ varies. However, the variation is not only due to the impact of sea -ice but also determined by other factors, such as atmospheric circulation. Therefore an approach capable of quantifying the influence of a factor is indispensable ~~to extract~~for extracting the corresponding ~~part~~contribution of sea -ice effect from the total heat flux change. To distinguish sea -ice's contribution from the other processes, the linkage between sea -ice and heat flux needs to be identified through either temporal correlation or spatial correlation, if the effect of sea -ice is assumed to be linear. A canonical case of the former is ~~the~~equilibrium feedback assessment (EFA)~~method,~~, which has been used to quantify the influence of sea -ice on cloud cover (Liu et al., 2012) and the heat flux response to SST (Frankignoul and Kestenare, 2002).

Here we adopt a method similar to EFA, but built on spatial correlation due to the limitation of data and computation. As a high-temporal-resolution CFRAM calculation, such as 6-hourly or daily, is computationally expensive, monthly data are used in the analysis. However, the monthly resolution is too coarse to explain the relationship between heat fluxes and sea-ice concentration by temporal correlations. Therefore, spatial correlations are calculated. This method is used in Hu et al. (2017) to correct cloud feedback. The response of heat flux to ~~change~~changes in sea -ice concentration (SIC) is represented as

$$F(s) = \lambda I(s) + N(s), \quad (4)2)$$

where $F(s)$ is the heat flux anomaly at location s , $I(s)$ is anomalous SIC, λ is the response coefficient of heat flux to SIC change, and $N(s)$ is the climate noise independent of SIC variability. The response coefficient can be calculated as

$$\lambda = \frac{cov[F(s), I(s)]}{cov[I(s), I(s)]}, \quad (2)3)$$

where $cov[F(s), I(s)]$ is the spatial covariance between heat flux and SIC, and $cov[I(s), I(s)]$ is the spatial variance of SIC.

The statistical significance of response coefficient is tested using a two-sided Student's t-test, where the effective degree of freedom is estimated from the auto-correlation function (Bretherton et al., 1999) as

$$n = N \frac{1-r_1 r_2}{1+r_1 r_2}, \quad (34)$$

where n is the effective degree of freedom, N is the sample size, and r_1 is the lag-one auto-correlation of heat flux ~~and~~ (similarly r_2 for SIC~~).~~ Note that auto-correlation of heat flux and SIC is so strong that r_1 and r_2 can approach 1, leading to a ~~drastieally~~drastic decrease of effective degree of freedom.

Unlike the ~~present earth~~modern Earth observation system, the Pliocene climate proxy data are reconstructed mainly from the ~~benthic~~benthic-oxygen isotope analysis of deep-sea samples, such as foraminifera, diatom, and ostracod assemblages. Several climate features have been revealed with the multi-proxy data, ~~one~~ (Haywood et al., 2016a). ~~One of the most concern is permanent El Niño-like condition during the mid Pliocene warm period (Wara et al., 2005; Federov et al, 2006), which points out that the SST difference between the western and eastern equatorial Pacific was absent or less evident, similar to the contemporary El Niño SST pattern while not happening on interannual timescale. The other characteristic concerning~~ is Arctic amplification — the warming in surface air temperature (SAT) in the Arctic region tends to be more than twice as warm as that in the low- and mid-latitude ~~region~~regions (Serreze and Barry, 2011). ~~However, the~~Furthermore, Arctic SAT and SST during Pliocene is significantly warmer than today ~~even though they have, despite~~ comparable CO₂ ~~concentration~~concentrations (Ballantyne et al., 2013), ~~which~~. This probably stems from the ~~fact that the~~ present transient process ~~that~~ has not yet reached a steady state, or is due to the change of ~~the~~ gateways that can affect the Atlantic meridional overturning circulation (AMOC) (Brierley and Fedorov, 2016; Otto-Bliesner et al., 2017; Feng et al., 2017).

In Figure 1, we show the ~~changes in annual mean warming and seasonal warming averaged over the Arctic Ocean for~~ SST and SAT between the ~~Pliocene and preindustrial period and the Pliocene epoch simulations~~. The shaded circles in the SST change distribution (Figure 1a) represent the mean annual SST anomalies at 95% confidence-assessed marine sites from ~~the~~ Deep Sea Drilling Project (~~DSDP~~) and Ocean Drilling Program (~~ODP~~), which are available in the supplementary table of Dowsett et al. (2012). ~~The overlay of proxy data over the filled contour maps does not show the difference well, so the difference of annual mean SST anomaly between EC-Earth simulation and the proxy data is shown in Figure S2.~~ In contrast to the large underestimation of multi-model ensembles ~~to~~regarding the warming over the northern Atlantic sector of the Arctic Ocean (Dowsett et al., 2012), the warming amplitude and pattern in EC-Earth simulation is comparable with the high-confidence proxy data. This is consistent with the ~~results~~result of Koenigk et al. (2013), which ~~pointed out~~suggests that the sea ice change in EC-Earth is strong and ~~that the~~ EC-Earth simulations show a strong Arctic amplification compared to most CMIP3 models. ~~Meanwhile, a warming can be seen along the coastal upwelling zones off the America, which implies a permanent El Niño-like feature.~~ According to Figure 1b, the Pliocene SAT north of 70 °N is as much as 10–18 °C higher than the preindustrial period, similar to the mid-Pliocene paleoclimate estimate by Robinson et al. (2008).

~~Figure~~Figures 1a and 1b also show that the SST and SAT anomaly patterns are somewhat similar over low- and mid-latitude ~~region, but they are apparently~~regions, different from over high-latitude ~~region~~regions, particularly over the Arctic Ocean, which ~~is~~was previously illustrated by Hill et al. (2014). This disparity results from the intense air–sea coupling over tropical and subtropical ~~ocean~~oceans, while the air–sea interaction is relatively weak over the Arctic Ocean owing to the albedo and insulation effects of sea ice. ~~Noteworthy, the~~Notably, SST warming ~~of SST~~ averaged over the Arctic Ocean shows a distinct seasonal evolution from that of SAT, ~~and~~; the maximum warming in SST occurs in summer, while the maximum warming in SAT happens during winter (FigureFigures 1c and 1d).

The SIC is very sensitive during the different period as shown in Figure 2a-e. During the preindustrial period, the annual mean sea ice appears to cover the whole Arctic Ocean except for the Greenland Sea, the Norwegian Sea, and the Barents Sea, and it retreats to the western Arctic Ocean in the Pliocene, leading to a significant decrease of sea ice extent over the Fram Basin and Baffin Bay (Figures 2a-c). Consequently, the net air-sea interface heat exchange at the surface of ice or ocean varies greatly (Figure 2d-f). The sea ice-f. The net heat flux and other flux terms mentioned hereafter are defined as positive downward. A positive value means that the ocean gains heat from the atmosphere and a negative value means oceanic heat loss. The net heat flux over the sea ice-covered area seems to be clearly shows net heat loss during both the preindustrial period and the Pliocene (Figures 2d and 2e). Thus, it can be expected that net heat gain will occur when the sea ice declines. However, the Fram Basin and Baffin Bay displays display pronounced heat loss, which might be linked to the disappearance of sea ice in the Pliocene (Figure 2b).

The net heat flux at the air-sea interfaces surface of ice or ocean can be written represented as

$$Q_{net} = Q_{sw} + Q_{lw} + Q_{sh} + Q_{lh}, \quad (4)$$

Where Q_{sw} and Q_{lw} are the sum of four terms: the net solar shortwave and radiative flux, the net longwave radiative heat fluxes, Q_{sh} and Q_{lh} are flux, the turbulent sensible heat flux, and the turbulent latent heat fluxes. All terms are defined positive downward. Therefore, the positive value means that ocean gains heat from the atmosphere and the negative value means oceanic heat loss.

Figure 3 compares the annual mean of the four components of surface heat flux terms to further illustrate the possible relationship between sea ice and net heat exchange (Figure Figures 2c and 2f). The radiative and turbulent heat fluxes flux anomalies both are positive over the Chukchi Sea, thereby indicating a marked net heat gain emerging there. Over the Beaufort Sea and East Siberian Sea, the positive change in the net shortwave radiation is anomalies are dominant over the other three negative components, yielding the net heat gain. On the contrary In contrast, the positive net shortwave radiation anomalies over the Fram Basin, the Greenland Sea, and Baffin Bay is are less than the sum of net longwave radiation and turbulent heat fluxes flux anomalies, thus leading to net heat loss. The negative turbulent heat fluxes flux anomalies over Fram Basin, the Greenland Sea, and Baffin Bay are so prominent, indicating the sea ice effect on turbulent heat fluxes flux anomalies in light of the transition to ice-covered or ice-free state states, respectively. As shown in Note that the partition threshold of ice-free and ice-covered conditions is 15% SIC, i.e., a grid point with an SIC of less than 15% is considered ice-free. In Figure 2c, the diagonal stripe represents the region with the transition from ice-covered to ice-free condition, and the diagonal crosshatch represents the region remaining that retains its ice-covered status as the simulation shifts from the preindustrial period to the Pliocene. Only ice-covered regions are examined, as there appears to be large surface heat flux changes in regions that contain no sea ice in both periods, which could be contaminating the statistical relationships between sea ice and the associated surface flux changes.

4 Albedo effect of sea -ice

Arctic amplification has been demonstrated by significant SAT anomalies in the foregoing Pliocene simulation, ~~and it can be accounted as the synergy of CO₂-external forcing and feedback effects associated with.~~ Similar to the process-based decomposition of a climate difference in Hu et al. (2017), the SAT anomalies in the Pliocene simulation as compared to the preindustrial simulation can be thought of as the combination of partial temperature perturbations due to radiative feedbacks (surface albedo, cloud, water vapour, and air temperature,) and non-radiative feedbacks (surface sensible and latent heat fluxes, dynamical advection, ocean processes, etc.). That is to say, the albedo effect of sea -ice and snow can be quantified by climate feedback analysis such as CFRAM. ~~The surface~~ Surface albedo is defined as the ratio ~~proportion~~ of the ~~reflected to the incoming incident~~ solar shortwave radiation that is reflected by the surface, therefore indicating that albedo effect is relevant ~~with to net~~ shortwave radiation rather than net longwave radiation and turbulent heat fluxes.

The annual mean net shortwave radiation change due to sea -ice and snow albedo derived from CFRAM is presented in Figure 4. The largest net shortwave radiation change exceeding 50 Wm^{-2} takes place over ~~the~~ Fram Basin and Baffin Bay, and most of the Arctic Ocean, except for part of ~~the~~ North Atlantic and the Barents Sea ~~show, shows net~~ shortwave radiative heat gain. ~~Comparing~~ Compared with the SIC change (Figure 2c), the increase of annual mean net shortwave radiation absorbed by the ocean is in accordance with sea -ice retreat, which can be clearly depicted in a scatter plot (Figure 5). ~~The high~~ The effective degree of freedom is calculated from Formula (4) for testing statistical significance, and the correlation coefficient ($r = -0.9284$) is significant at a 99% confidence level. This indicates that changes in sea -ice extent can explain the approximate 84.71% (square of correlation coefficient) variance of total shortwave radiation change due to albedo, and the residual variance may be caused by changes in snow cover ~~or and~~ sea -ice/snow state as well as thickness. The statistically significant response coefficient calculated according to formula (23) is ~~-46.5-43.0~~ Wm^{-2} ~~(exceeding 99% confidence level),~~ indicating that a 1% decrease in annual mean SIC leads to an approximate 0.543 Wm^{-2} increase in net shortwave radiative heat flux at the surface.

~~Regarding the seasonal variation of~~ As SIC and ~~the~~ incoming solar radiation ~~are distinct~~ in the polar region vary with season, we examine the response of net shortwave radiation to sea -ice change for every month. As shown in Figure 6, the response coefficient of albedo to SIC displays a seasonal variation, peaking in ~~which it peaks in May~~ June with ~~the~~ maximum absolute value ~~188.4 of 178.3~~ Wm^{-2} (approximate 21.8 Wm^{-2} increase in net shortwave radiation due to 1% decrease in SIC). The prominent oceanic heating in May and June seems ~~inconsistent~~ consistent with the maximum SST warming in August, as the response of seawater lags about 2 months behind due to the great heat inertia and heat capacity of seawater (Venegas et al., 1997; Zheng et al., 2014). Even though Arctic sea -ice itself has a great variability owing to melting and freezing processes, ~~the~~ SIC anomalies do not exhibit a large variability in different seasons, ranging from 0.3419 to 0.4426 as shown in the standard deviation of SIC (Table 1). However, the standard deviation of net shortwave radiation anomalies (with respect to monthly mean) associated with albedo effect varies from 88.4352.45 Wm^{-2} in May to 0 Wm^{-2} in December, when the polar night ~~occurring~~ occurs without any sunlight. Moreover, ~~it is found from our~~ correlation analysis

indicates that sea -ice has a statistically significant impact on surface shortwave radiation, except in November, December, and January, when there is low incident solar shortwave radiation during the Arctic winter. Overall, the seasonality of sea ice's albedo effect of sea-ice on surface shortwave radiation is attributed primarily to the seasonal cycle of net shortwave radiation, and the contribution of sea-ice SIC variation is substantially small.

5 Insulation effect of sea -ice

5.1 Insulation effect of sea -ice on surface radiation

The insulating effect of sea -ice, has an indirect effect on the net surface shortwave and longwave fluxes. By separating the overlying atmosphere from the ocean, does not affect surface shortwave or longwave radiation directly. In fact, the insulation sea ice reduces the evaporation from the ocean to atmosphere, resulting in a decrease of in water vapour and cloud cover, and thus playing. This reduction plays a non-negligible role on in the amount of downward shortwave and longwave radiation reaching the surface radiation. However, the water vapour and cloud contain a mixture of local evaporation and remote moisture transport. In also affects water vapour and cloud amount. Thus, in order to address the insulation effect of sea -ice, two steps have to be performed. First, we obtain the total influence of water and cloud on surface radiation by CFRAM. Second, we need to extract the contribution from a local source associated with sea -ice.

Figure 7 shows the annual mean cloud feedback and water vapour feedback on net shortwave and longwave radiation, respectively, before removing the remote effects on clouds and water vapour. Even though the an increase in cloud cover is expected with the diminishing Arctic sea -ice (Liu et al., 2012), whether the increased cloud cover will heat or cool the surface depends on the cloud characteristics of cloud. The cloud feedback on shortwave radiation is nearly out of phase with that on longwave radiation, except in the Beaufort Sea and the East Siberian Sea (Figure 7a, 7b). The significant decrease of low cloud cover in the North Atlantic (Figure S3a) may enhance incoming shortwave radiation and weaken downwelling longwave radiation, thus contributing to the positive anomaly in shortwave radiation and negative anomaly in longwave radiation in the North Atlantic. Similarly, the increase of high cloud cover east and north of Greenland (Figure S3b) is responsible for the positive anomaly in longwave radiation over the related areas. In contrast, the water vapour feedback tends to simultaneously cool and heat the surface by absorbing solar radiation and heat the surface by downwelling longwave radiation, and respectively; the latter heating is one order of magnitude higher than the former cooling (Figure 7c, 7d).

The approach to extract the counterpart of sea-ice local insulation effect due to changes in sea ice concentration is based on the premise that the insulation effect on surface radiation is linear with SIC. Like the steps performed into isolate the albedo effect, the response coefficient of shortwave and longwave radiation due to cloud and water vapour for annual mean and seasonal evolution can be calculated respectively, and the results are shown in Figure 8. As to In the annual mean, the main contributor comes from cloud feedback on longwave radiation ($-12.6(-11.1 \text{ Wm}^{-2})$), and the cloud feedback on shortwave radiation and water vapour feedback on longwave radiation are similar in magnitude, but opposite in sign. In addition, the annual mean absorption of incoming solar radiation by water vapour is negligible, and this is true for the

individual month as well. The absorption and reflection of shortwave radiation by cloud ~~represents~~ shows a pronounced seasonal cycle, with a large effect in July and August. However, there is no statistically significant relationship between SIC and cloud feedback on shortwave radiation and SIC (Table 2). Comparing Compared to the seasonal variation of shortwave radiation change, standard deviation of the net shortwave radiation anomalies, standard deviation of the net longwave radiation anomalies caused by cloud and water vapour associated with local SIC anomalies both show smaller seasonal variation, therefore leading to a relatively constant contribution of sea-ice insulation to surface longwave radiation, except in summer months when there is a lack of significant interaction linear relationship between SIC and longwave radiation (Table 2). Note that the longwave cloud forcing in September (-17.6 Wm^{-2}) is quite large relative to all the other months, which might result from the maximum cloud cover over the Arctic, as well as the fact that the linear relationship between sea ice concentration and longwave radiation changes due to cloud is strongest in September.

5.2 Insulation effect of sea-ice on turbulent heat fluxes

The air-sea turbulent heat fluxes, including sensible and latent heat fluxes, have been widely studied with the bulk aerodynamic formula, which specifies that the turbulent heat fluxes are dependent on surface wind speed, sea surface and air temperature difference, specific humidity difference, and the bulk heat transfer coefficient. However, due to the existence of sea-ice, the Arctic turbulent heat fluxes show distinctive features from ice-free conditions, which has been mentioned in Section 3. It is therefore essential to take the insulation effect of sea-ice into account and differentiate ice-covered fluxes from ice-covered versus ice-free areas. This is demonstrated in Figure 9, which displays the Pliocene anomalies in annual mean sensible and latent heat flux change fluxes as a function of SIC anomalies. There are is a larger spread of spread in the turbulent heat flux change anomalies over the ice-free areas (grey symbols, corresponding to the diagonal hatched region in Figure 2c) than that of in anomalies from the ice-covered areas (light blue symbols, cross-hatched region in Figure 2c) because the former is free from the constraint of sea-ice. The constraint of sea-ice can be apparently captured through the scatter plot of turbulent heat flux and changes in SIC change (the light blue plot in Figure 9, corresponding to the diagonal crosshatch symbols). For the ice-covered areas in Figure 2c, and, SIC can explain approximate 59% and 74% (square of correlation coefficient) of the variance in the sensible heat flux and latent heat flux, respectively.

The linear regressions of sensible and latent heat flux anomalies on SIC are similar but different. The response coefficient of sensible heat flux (35.3 Wm^{-2}) to SIC is larger than that of latent heat flux (27.7 Wm^{-2}), for the ice-covered areas, which means that the sensible heat flux is more sensitive to SIC change than the latent heat flux. Noteworthy Notably, this is different from the turbulent heat flux variability over low- and mid-latitude regions, where the trend variability of sensible heat flux is significantly less than that of latent heat flux (e.g., such as the trend of turbulent heat flux over the low- and mid-latitude North Pacific and North Atlantic oceans from 1984–2004 (Li et al., 2011)). The positive intercept on the turbulent flux anomaly axis implies more heat gain at the sea surface, even if there is now without SIC change. Because the large specific heat capacity of seawater leads to less warming of the ocean than of the atmosphere, therefore the sea surface and air temperature difference or (the specific humidity difference) decreases induring the cold season when the turbulent

heat transport is the most pronounced, and consequently resulting in the lessa lower annual heat loss from the ocean to the atmosphere.

Figure 10 shows the seasonal response coefficient of the sensible and latent heat fluxes to the sea-ice. Apparently two SIC. It appears that the turbulent heat fluxes have thea similar seasonal evolution, peaking in November and showing a negative response in July. Therefore the maximum warming of SAT occurs in November as a consequence of, the prompt atmospheric prompt response to turbulent heating is an important contributing factor to the maximum SAT warming that occurs in November. The melting of sea-ice due to warming by high levels of CO₂ can attenuate the insulation effect and result in more heat transfer through the processes of conduction or evaporation from the ocean to the atmosphere when SST is higher than SAT; therefore, the turbulent heat fluxes correlate positively with SIC in all seasons except summer (Table 3). If SAT is higher than SST, (for instance, in July the), sea -ice will inhibit the heat transfer from the atmosphere to ocean; thus, the negative correlation emerges. However, the correlations between the turbulent heat fluxes and SIC in summer are not statistically significant (Table 3), indicating other factors might be dominant rather than sea -ice might be dominant.

6 Summary and discussion

In the present work we attempt to understand the albedo and insulation effects of sea-ice, on a warm Arctic climate during Pliocene simulated by EC-Earth coupled model. In contrast to Arctic amplification in the Pliocene has previously been addressed from reconstructed data (e.g. Robinson et al., 2008; Brigham-Grette et al., 2013); however these data tell only part of the story because of a scarcity of data sites. A model may be applied to investigate mechanisms and processes that help understanding. In contrast to the underestimation of multi-model ensembles documented in Dowsett et al. (2012), the EC-Earth Pliocene simulation can better display some main features manifested in the characteristics that have been revealed by the paleoclimate proxy data from deep-sea oxygen isotope analysis. Thus the EC-Earth coupled model is used in the present work to simulate the Pliocene climate and study the contribution of sea ice albedo and insulation to Arctic amplification in Pliocene had been confirmed by reconstructed data (e.g. Robinson et al., 2008; Brigham-Grette et al., 2013). Proxy data, however, tell only part of the story. Thus a model is applied and it can reveal the complete picture with reasonable explanation.

As a key to reveal the important features of Arctic amplification, the air-Air-sea heat flux variation in response to Arctic sea -ice change is quantitatively assessed by CFRAM and an EFA-like method: in order to reveal important features of Arctic amplification. Table 4 summarizes the results presented in sectionSections 4 and 5, which separately illustratedillustrate the effects of changes in albedo and insulation of sea -ice on surface heat exchange. Annual mean and seasonal evolution of effects are both considered, and. These allow us to partly interpret the mechanisms of Arctic amplification because the results are merely the contribution from sea -ice change. A complete energy budget, including dynamical and thermodynamical processes, is required to understand Arctic amplification comprehensively. The Pliocene Arctic amplification compared to the preindustrial simulation represents a maximum SST warming in August and expected to partly interpret the variability of heat flux.

390 —~~The albedo~~ maximum SAT warming in November, which might be associated with the albedo and insulation effects of sea ice. Albedo only regulates the shortwave radiation, and its effect is primarily determined by annual cycle of insolation. As sea -ice melts ~~from starting in~~ early spring, the enhanced insolation through open sea surface makes the ocean warmer, with the most pronounced heating anomalies in May and June. Because of the great heat inertia and heat capacity of seawater, the SST warming anomaly peaks in August. As a result of the albedo effect of sea -ice, ocean heat content increases and more heat is stored in the upper ocean, which is the potential for the later enhanced heat release from ocean to atmosphere. The insulation effect of sea -ice can indirectly modulate ~~not only~~ shortwave and longwave radiation anomalies indirectly through cloud and water vapour, ~~but also as well as directly modulate~~ sensible and latent heat ~~fluxes directly flux~~ anomalies, since sea -ice serves as a barrier. Averaged over the year, the absorption of longwave radiation due to insulation effect is about 4 times stronger than the reflected shortwave radiation by cloud, while the contribution of water vapour to shortwave radiation is almost negligible. The longwave radiation change anomalies in response to cloud and water vapour is attributed to downwelling longwave radiation, as upwelling longwave radiation depends solely on the surface temperature according to the Stefan–Boltzmann law, and its seasonal variation is relatively small compared to the significant seasonality ~~showing~~ in shortwave radiation. The Pliocene sea -ice decline ~~accelerates, as compared to the preindustrial period, amplifies~~ the turbulent exchange between the ocean and atmosphere, and the annual sum of sensible and latent heat ~~fluxes exceed flux~~ anomalies exceeds radiation ~~fluxes flux anomalies~~. In particular, heat is released to the atmosphere by the prominent enhanced turbulent heat ~~fluxes flux anomalies~~ in winter, ~~amplifying the atmospheric warming~~ November, contributing to the formation of the maximum SAT anomaly in November.

400 A synthesis of Arctic amplification given by Serreze and Barry (2011) has introduced some of the physical processes mentioned above, including sea ice loss, albedo feedback, cloud cover, and water vapour. Unlike Serreze and Barry (2011), in this work we apply CFRAM and an EFA-like method to untangle these physical processes and obtain a quantitative understanding of sea-ice effects, which would help to directly evaluate the impact on heat exchange once the sea-ice concentration variation within Arctic is given. The EC-Earth simulation shows a stronger Arctic amplification than multi-model ensembles (Dowsett et al., 2012). However, an underestimation of Arctic warming as compared to proxy data remains in the EC-Earth simulation, implying less warmth produced by the EC-Earth model from oceanic heat transport, which yields a clue for improving the simulation. Furthermore, caution should be exercised when discussing sea-ice effects on heat flux, as underestimating Arctic warming might affect the interface heat exchange.

415 Though significant albedo and insulation effects of sea -ice have been studied, the possible nonlinear response of heat flux to sea -ice can not be captured in this work. In addition, ~~the this~~ approach to ~~extract extracting~~ sea -ice effects is based on ~~the~~ spatial correlation; whether the corresponding conclusion is consistent with that from EFA ~~method~~ remains uncertain. The consistency check is computationally expensive for CFRAM calculation, as ~~the~~ EFA requires high temporal resolution. The present study is based on the Pliocene simulation with the EC-Earth, and the results may be model-dependent. Further work is needed to compare our results with other PlioMIP models.

Acknowledgements. This work was supported by the Swedish Research Council VR for the Swedish–French project GIWA, the China Scholarship Council (Grant 201606345010), and the Opening Project of Key Laboratory of Meteorological Disaster of Ministry of Education of Nanjing University of Information Science and Technology (Grant KLME1401). The EC-Earth mid-Pliocene simulation ~~is~~was performed at ECMWF's computing and archive facilities, and the analysis ~~are~~was performed on resources provided by the Swedish National Infrastructure for Computing (SNIC) at Linköping University.

References

- Alexander, M.A., Bhatt, U.S., Walsh, J.E., Timlin, M.S., Miller, J.S. and Scott, J.D.: The atmospheric response to realistic Arctic sea ice anomalies in an AGCM during winter, *J. Climate*, 17, 890-905, doi:10.1175/1520-0442(2004)017<0890:TARTRA>2.0.CO;2, 2004.
- Alexeev, V.A., Ivanov, V.V., Kwok, R. and Smedsrud, L.H.: North Atlantic warming and declining volume of arctic sea ice, *The Cryosphere Discussions*, 7, 245-265, doi:10.5194/tcd-7-245-2013, 2013.
- Ballantyne, A.P., Axford, Y., Miller, G.H., Otto-Bliesner, B.L., Rosenbloom, N. and White, J.W.: The amplification of Arctic terrestrial surface temperatures by reduced sea-ice extent during the Pliocene, *Palaeogeogr. Palaeoclimatol. Palaeoecol.*, 386, 59-67, doi:10.1016/j.palaeo.2013.05.002, 2013.
- Balsamo, G., Beljaars, A., Scipal, K., Viterbo, P., van den Hurk, B., Hirschi, M. and Betts, A.K.: A revised hydrology for the ECMWF model: Verification from field site to terrestrial water storage and impact in the Integrated Forecast System, *J. Hydrometeorol.*, 10, 623-643, doi:10.1175/2008JHM1068.1, 2009.
- Bintanja, R. and Selten, F.M.: Future increases in Arctic precipitation linked to local evaporation and sea-ice retreat, *Nature*, 509, 479-482, doi:10.1038/nature13259, 2014.
- Bretherton, C.S., Widmann, M., Dymnikov, V.P., Wallace, J.M. and Bladé, I.: The effective number of spatial degrees of freedom of a time-varying field, *J. Climate*, 12, 1990-2009, doi:10.1175/1520-0442(1999)012<1990:TENOSD>2.0.CO;2, 1999.
- Brierley, C. M. and Fedorov, A. V.: Comparing the impacts of Miocene–Pliocene changes in inter-ocean gateways on climate: Central American Seaway, Bering Strait, and Indonesia, *Earth Planet. Sci. Lett.*, 444, 116-130, doi:10.1016/j.epsl.2016.03.010, 2016.
- Brigham-Grette, J., Melles, M., Minyuk, P., Andreev, A., Tarasov, P., DeConto, R. and Haltia, E.: Pliocene warmth, polar amplification, and stepped Pleistocene cooling recorded in NE Arctic Russia. *Science*, 340, 1421, doi:10.1126/science.1233137, 2013.
- Burt, M.A., Randall, D.A. and Branson, M.D.: Dark warming, *J. Climate*, 29, 705-719, doi:10.1175/JCLI-D-15-0147.1, 2016.

- 455 Dowsett, H.J., Robinson, M.M., Haywood, A.M., Hill, D.J., Dolan, A.M., Stoll, D.K., Abe-Ouchi, A., Chandler, M.A.,
Rosenbloom, N.A., Otto-Bliesner, B.L. and Bragg, F.J.: Assessing confidence in Pliocene sea surface temperatures to
evaluate predictive models, *Nat. Clim. Change*, 2, 365-371, doi:10.1038/nclimate1455, 2012.
- Dowsett, H., Dolan, A., Rowley, D., Moucha, R., Forte, A. M., Mitrovica, J. X., Pound, M., Salzmann, U., Robinson, M.,
Chandler, M., Foley, K., and Haywood, A.: The PRISM4 (mid-Piacenzian) paleoenvironmental reconstruction, *Clim. Past*,
460 12, 1519-1538, doi:10.5194/cp-12-1519-2016, 2016.
- Fedorov, A.V., Dekens, P.S., McCarthy, M., Ravelo, A.C., Barreiro, M., Pacanowski, R.C. and Philander, S.G.: The
Pliocene paradox (mechanisms for a permanent El Niño), *Science*, 312, 1485-1489, doi:10.1126/science.1122666, 2006.
- Feng, R., Otto-Bliesner, B. L., Fletcher, T. L., Tabor, C. R., Ballantyne, A. P., & Brady, E. C.: Amplified Late Pliocene
terrestrial warmth in northern high latitudes from greater radiative forcing and closed Arctic Ocean gateways, *Earth Planet.
Sci. Lett.*, 466, 129-138, doi:10.1016/j.epsl.2017.03.006, 2017.
- 465 Frankignoul, C. and Kestenare, E.: The surface heat flux feedback. Part I: estimates from observations in the Atlantic and the
North Pacific, *Clim. Dynam.*, 19, 633-647, doi:10.1007/s00382-002-0252-x, 2002.
- Fu, Q. and Liou, K.N.: Parameterization of the radiative properties of cirrus clouds, *J. Atmos. Sci.*, 50, 2008-2025,
doi:10.1175/1520-0469(1993)050<2008:POTRPO>2.0.CO;2, 1993.
- 470 Gaetani, M., Messori G., Zhang Q., Flamant C., and Pausata F.S.: Understanding the mechanisms behind the northward
extension of the West African Monsoon during the Mid-Holocene. *J. Climate*, doi:10.1175/JCLI-D-16-0299.1, 2017.
- Gildor, H., Ashkenazy, Y., Tziperman, E. and Lev, I.: The role of sea ice in the temperature-precipitation feedback of glacial
cycles, *Clim. Dynam.*, 43, 1001-1010, doi:10.1007/s00382-013-1990-7, 2014.
- Graversen, R.G. and Burtu, M.: Arctic amplification enhanced by latent energy transport of atmospheric planetary waves, *Q.
J. Roy. Meteor. Soc.*, 142, 2046-2054, doi:10.1002/qj.2802, 2016.
- 475 Haywood, A.M., Dowsett, H.J. and Dolan, A.M.: Integrating geological archives and climate models for the mid-Pliocene
warm period, *Nat. Commun.*, 7, 1-14, doi:10.1038/ncomms10646, 2016a.
- Haywood, A.M., Dowsett, H.J., Dolan, A.M., Chandler, M.A., Hunter, S.J. and Lunt, D.J.: The Pliocene Model
Intercomparison Project (PlioMIP) Phase 2: scientific objectives and experimental design, *Clim. Past*, 12, 663-675,
480 doi:10.5194/cp-12-663-2016, 2016b.
- Hazeleger, W., Wang, X., Severijns, C., Ștefănescu, S., Bintanja, R., Sterl, A., Wyser, K., Semmler, T., Yang, S., Van den
Hurk, B. and Van Noije, T.: EC-Earth V2. 2: description and validation of a new seamless earth system prediction model,
Clim. Dynam., 39, 2611-2629, doi:10.1007/s00382-011-1228-5, 2012.
- Hill, D.J., Haywood, A.M., Lunt, D.J., Hunter, S.J., Bragg, F.J., Contoux, C., Stepanek, C., Sohl, L., Rosenbloom, N.A.,
485 Chan, W.L. and Kamae, Y.: Evaluating the dominant components of warming in Pliocene climate simulations, *Clim. Past*,
10, 79-90, doi:10.5194/cp-10-79-2014, 2014.
- Hu, X., Li, Y., Yang, S., Deng, Y. and Cai, M.: Process-based Decomposition of the Decadal Climate Difference between
2002-13 and 1984-95, *J. Climate*, 30, 4373-4393, doi:10.1175/JCLI-D-15-0742.1, 2017.

- Kageyama, M., Braconnot, P., Harrison, S. P., Haywood, A. M., Jungclauss, J. H., Otto-Bliesner, B. L., Peterschmitt, J.-Y.,
 490 Abe-Ouchi, A., Albani, S., Bartlein, P. J., Brierley, C., Crucifix, M., Dolan, A., Fernandez-Donado, L., Fischer, H.,
 Hopcroft, P. O., Ivanovic, R. F., Lambert, F., Lunt, D. J., Mahowald, N. M., Peltier, W. R., Phipps, S. J., Roche, D. M.,
 Schmidt, G. A., Tarasov, L., Valdes, P. J., Zhang, Q., and Zhou, T.: The PMIP4 contribution to CMIP6 – Part 1: Overview
 and over-arching analysis plan, *Geosci. Model Dev.*, 11(3), 1033-1057, doi:10.5194/gmd-11-1033-2018, 2018.
- Kim, K.Y., Hamlington, B.D., Na, H. and Kim, J.: Mechanism of seasonal Arctic sea ice evolution and Arctic amplification,
 495 *The Cryosphere*, 10(5), 2191-2202, doi:10.5194/tc-10-2191-2016, 2016.
- Koenigk, T., Brodeau, L., Graverson, R. G., Karlsson, J., Svensson, G., Tjernström, M. and Wyser, K.: Arctic climate change
 in 21st century CMIP5 simulations with EC-Earth, *Climate dynamics*, 40(11-12), 2719-2743, doi: 10.1007/s00382-012-
 1505-y, 2013.
- Krumpen, T., Gerdes, R., Haas, C., Hendricks, S., Herber, A., Selyuzhenok, V., Smedsrud, L. and Spreen, G.: Recent
 500 summer sea ice thickness surveys in Fram Strait and associated ice volume fluxes, *The Cryosphere*, 10, 523-534,
 doi:10.5194/tc-10-523-2016, 2016.
- Lang, A., Yang, S. and Kaas, E.: Sea-ice thickness and recent Arctic warming, *Geophys. Res. Lett.*, 44, 409-418,
 doi:10.1002/2016GL071274, 2017.
- Li, C., Notz, D., Tietsche, S. and Marotzke, J.: The transient versus the equilibrium response of sea ice to global warming,
 505 *J.Climate*, 26, 5624-5636, doi:10.1175/JCLI-D-12-00492.1, 2013.
- Li, G., Ren, B., Zheng, J. and Yang, C.: Net air–sea surface heat flux during 1984–2004 over the North Pacific and North
 Atlantic oceans (10N–50N): annual mean climatology and trend, *Theor. Appl. Climatol.*, 104, 387-401, doi:
 10.1007/s00704-010-0351-2, 2011.
- Liu, Y., Key, J.R., Liu, Z., Wang, X. and Vavrus, S.J.: A cloudier Arctic expected with diminishing sea ice, *Geophys. Res.*
 510 *Lett.*, 39, L05705, doi:10.1029/2012GL051251, 2012.
- Lu, J. and Cai, M.: A new framework for isolating individual feedback processes in coupled general circulation climate
 models. Part I: Formulation, *Clim. Dynam.*, 32, 873–885, doi:10.1007/s00382-008-0425-3, 2009.
- Madec, G.: “NEMO ocean engine”. Note du Pole de mode ‘lisation, Institut Pierre-Simon Laplace (IPSL), France, No 27
 ISSN no 1288-1619, 2008.
- 515 Matthiessen, J., Knies, J., Vogt, C. and Stein, R.: Pliocene palaeoceanography of the Arctic Ocean and subarctic seas, *Philos.*
Trans. R. Soc. A., 367, 21–48, doi: 10.1098/rsta.2008.0203, 2009.
- Muschitiello, F., Zhang, Q., Sundqvist, H.S., Davies, F.J. and Renssen, H.: Arctic climate response to the termination of the
 African Humid Period, *Quat. Sci. Rev.*, 125, 91-97, doi:10.1016/j.quascirev.2015.08.012, 2015.
- Nghiem, S.V., Rigor, I.G., Perovich, D.K., Clemente - Colón, P., Weatherly, J.W. and Neumann, G.: Rapid reduction of
 520 Arctic perennial sea ice, *Geophys. Res. Lett.*, 34, L19504, doi:10.1029/2007GL031138, 2007.
- Otto-Bliesner, B. L., Jahn, A., Feng, R., Brady, E. C., Hu, A. and Löfverström, M.: Amplified North Atlantic warming in
 the late Pliocene by changes in Arctic gateways, *Geophys. Res. Lett.*, 44(2), 957-964, doi:10.1002/2016GL071805, 2017.

- Overland J.E., Wang M., Walsh J.E., Christensen J.H., Kattsov V.M., Champan W.L.: Climate model projections for the Arctic. In: AMAP (2011) Snow, Water, Ice and Permafrost in the Arctic (SWIPA): Climate Change and the Cryosphere. Arctic Monitoring and Assessment Programme (AMAP), Oslo, Norway. Xii, 538 pp, 2011.
- Pausata, F.S., Messori, G. and Zhang, Q.: Impacts of dust reduction on the northward expansion of the African monsoon during the Green Sahara period, *Earth Planet. Sci. Lett.*, 434, 298-307, doi:10.1016/j.epsl.2015.11.049, 2016.
- Pausata, F.S., Emanuel, K.A., Chiacchio, M., Diro, G.T., Zhang, Q., Sushama, L., Stager, J.C. and Donnelly, J.P.: Tropical cyclone activity enhanced by Sahara greening and reduced dust emissions during the African Humid Period, *Proc. Natl. Acad. Sci.*, 114, 6221-6226, doi:10.1073/pnas.1619111114, 2017a.
- Pausata, F.S., Zhang, Q., Muschitiello, F., Lu, Z., Chafik, L., Niedermeyer, E.M., Stager, J.C., Cobb, K.M. and Liu, Z.: Greening of the Sahara suppressed ENSO activity during the mid-Holocene, *Nat. Commun.*, 8, 1-12, doi:10.1038/ncomms16020, 2017b.
- Pithan, F. and Mauritsen, T.: Arctic amplification dominated by temperature feedbacks in contemporary climate models, *Nat. Geosci.*, 7, 181-184, doi:10.1038/ngeo2071, 2014.
- Robinson, M.M., Dowsett, H.J. and Chandler, M.A.: Pliocene role in assessing future climate impacts, *EOS, Trans. Am. Geophys. Union*, 89, 501-502, doi:10.1029/2008EO490001, 2008.
- Serreze, M.C., Barrett, A.P., Stroeve, J.C., Kindig, D.N. and Holland, M.M.: The emergence of surface-based Arctic amplification, *The Cryosphere*, 3, 11-19, doi:10.5194/tc-3-11-2009, 2009.
- Serreze, M.C. and Barry, R.G.: Processes and impacts of Arctic amplification: A research synthesis, *Glob. Planet. Chang.*, 77, 85-96, doi:10.1016/j.gloplacha.2011.03.004, 2011.
- Sévellec, F., Fedorov, A.V. and Liu, W.: Arctic sea-ice decline weakens the Atlantic Meridional Overturning Circulation, *Nat. Clim. Change*, 7, 604-610, doi:10.1038/nclimate3353, 2017.
- Shine, K.P. and Henderson-Sellers, A.: The sensitivity of a thermodynamic sea ice model to changes in surface albedo parameterization. *Journal of Geophysical Research*, 90, 2243–2250, 1985.
- Soden, B. J. and Held, I. M.: An assessment of climate feedbacks in coupled ocean–atmosphere models, *J. Climate*, 19, 3354–3360, doi:10.1175/JCLI3799.1., 2006.
- Song, X. and Zhang, G.J.: Role of climate feedback in El Niño–like SST response to global warming, *J. Climate*, 27, 7301–7318, doi:10.1175/JCLI-D-14-00072.1, 2014.
- Taylor, P.C., Cai, M., Hu, A., Meehl, J., Washington, W. and Zhang, G.J.: A decomposition of feedback contributions to polar warming amplification. *J. Climate*, 26, 7023-7043, doi:10.1175/JCLI-D-12-00696.1, 2013.
- Valcke, S.: OASIS3 user guide (prism_2-5), PRISM report series, no 2, 6th edn., 2006.
- Vancoppenolle, M., Fichefet T., Goosse H., Bouillon S., Madec G. and Maqueda M. A.: Simulating the mass balance and salinity of Arctic and Antarctic sea ice. 1. Model description and validation, *Ocean Modelling*, 27, 33-53, doi:10.1016/j.oceanmod.2008.10.005., 2009.

- Venegas, S. A., Mysak, L. A. and Straub, D. N.: Atmosphere–ocean coupled variability in the South Atlantic. *J. Climate*, 10(11), 2904-2920, doi:10.1175/1520-0442(1997)010<2904:AOCVIT>2.0.CO;2, 1997.
- Vihma, T.: Effects of Arctic sea ice decline on weather and climate: a review. *Surv. Geophys.*, 35, 1175-1214, doi:10.1007/s10712-014-9284-0, 2014.
- 560 Wara, M.W., Ravelo, A.C. and Delaney, M.L.: Permanent El Niño-like conditions during the Pliocene warm period. *Science*, 309, 758-761, doi:10.1126/science.1112596, 2005.
- Wetherald, R. T. and Manabe S.: Cloud feedback processes in a general circulation model. *J. Atmos. Sci.*, 45, 1397–1416, doi:10.1175/1520-0469(1988)045<1397:CFPIAG>2.0.CO;2., 1988.
- Winton, M.: Sea ice–albedo feedback and nonlinear Arctic climate change. Arctic sea ice decline: Observations, projections, mechanisms, and implications, 111-131, doi:10.1029/180GM09, 2008.
- 565 Zheng, J., Ren, B., Li, G. and Yang, C.: Seasonal dependence of local air-sea interaction over the tropical Western Pacific warm pool. *J. Trop. Meteorol.*, 20(4), 360-367, doi:10.16555/j.1006-8775.2014.04.009, 2014.

570

575

580

585

590

Table 1. The spatial standard deviation of SIC anomalies σ_{SIC} and **net** shortwave radiation anomalies due to albedo effect $\sigma_{\text{SW-albedo}}$ (Wm^{-2}) over the Arctic Ocean. $r_{\text{SW-albedo}}$ is **the** correlation coefficient between SIC and shortwave radiation anomalies. Those significant at **a** 99% confidence level are bolded.

	Jan	Feb	Mar	Apr	May	Jun	Jul	Aug	Sep	Oct	Nov	Dec
σ_{SIC}	<u>0.4425</u>	<u>0.4426</u>	<u>0.4426</u>	<u>0.4326</u>	<u>0.4325</u>	<u>0.3923</u>	<u>0.3423</u>	<u>0.3620</u>	<u>0.3919</u>	<u>0.3825</u>	<u>0.4025</u>	<u>0.4325</u>
$\sigma_{\text{SW-albedo}}$	<u>0.0301</u>	<u>1.550</u>	<u>11.095</u>	<u>42.792</u>	<u>88.435</u>	<u>80.374</u>	<u>41.882</u>	<u>29.851</u>	<u>15.066</u>	<u>3.592</u>	<u>0.2021</u>	0
		<u>75</u>	<u>.81</u>	<u>5.34</u>	<u>2.45</u>	<u>8.79</u>	<u>6.28</u>	<u>2.39</u>	<u>.85</u>	<u>16</u>		
$r_{\text{SW-albedo}}$	<u>—</u>	<u>—</u>	<u>—</u>	<u>—</u>	<u>—</u>	<u>—</u>	<u>—</u>	<u>—</u>	<u>—</u>	<u>—</u>	<u>—</u>	/
	<u>0.2522</u>	<u>0.4337</u>	<u>0.7563</u>	<u>0.8877</u>	<u>0.9080</u>	<u>0.9185</u>	<u>0.9085</u>	<u>0.9383</u>	<u>0.8857</u>	<u>0.5053</u>	<u>0.2511</u>	

595

Table 2. The spatial standard deviation of shortwave and longwave radiation anomalies due to cloud change ($\sigma_{\text{SW-cloud}}$, $\sigma_{\text{LW-cloud}}$) (Wm^{-2}) and water vapour change ($\sigma_{\text{SW-WV}}$, $\sigma_{\text{LW-WV}}$) (Wm^{-2}) over the Arctic Ocean. $r_{\text{SW-cloud}}$, $r_{\text{LW-cloud}}$, $r_{\text{SW-WV}}$ and $r_{\text{LW-WV}}$ are correlation coefficients between SIC and shortwave and longwave radiation anomalies due to cloud and water change, respectively. Those significant at **a** 99% confidence level are bolded. Here, **a** the cloud and water vapour change is specified as the part caused by sea -ice decrease.

	<u>Annual</u>	<u>Jan</u>	<u>Feb</u>	<u>Mar</u>	<u>Apr</u>	<u>May</u>	<u>Jun</u>	<u>Jul</u>	<u>Aug</u>	<u>Sep</u>	<u>Oct</u>	<u>Nov</u>	<u>Dec</u>
<u>$\sigma_{\text{SW-cloud}}$</u>	<u>4.76</u>	<u>0.01</u>	<u>0.16</u>	<u>1.11</u>	<u>3.86</u>	<u>5.97</u>	<u>11.71</u>	<u>19.61</u>	<u>13.86</u>	<u>3.21</u>	<u>0.50</u>	<u>0.04</u>	<u>0</u>
<u>$r_{\text{SW-cloud}}$</u>	<u>0.18</u>	<u>0.14</u>	<u>0.22</u>	<u>0.36</u>	<u>0.36</u>	<u>0.16</u>	<u>0.01</u>	<u>0.05</u>	<u>0.24</u>	<u>0.26</u>	<u>0.25</u>	<u>0.32</u>	/
<u>$\sigma_{\text{LW-cloud}}$</u>	<u>8.02</u>	<u>9.13</u>	<u>9.29</u>	<u>8.25</u>	<u>7.64</u>	<u>10.20</u>	<u>11.91</u>	<u>15.11</u>	<u>13.56</u>	<u>11.96</u>	<u>10.01</u>	<u>10.18</u>	<u>9.86</u>
<u>$r_{\text{LW-cloud}}$</u>	<u>-0.46</u>	<u>-0.59</u>	<u>-0.56</u>	<u>-0.56</u>	<u>-0.51</u>	<u>-0.36</u>	<u>0.06</u>	<u>0.04</u>	<u>-0.23</u>	<u>-0.54</u>	<u>-0.41</u>	<u>-0.60</u>	<u>-0.56</u>
<u>$\sigma_{\text{SW-WV}}$</u>	<u>0.29</u>	<u>0.001</u>	<u>0.03</u>	<u>0.14</u>	<u>0.40</u>	<u>0.59</u>	<u>0.85</u>	<u>0.85</u>	<u>0.63</u>	<u>0.33</u>	<u>0.09</u>	<u>0.01</u>	<u>0</u>
<u>$r_{\text{SW-WV}}$</u>	<u>-0.02</u>	<u>-0.05</u>	<u>0.02</u>	<u>0.06</u>	<u>0.05</u>	<u>0.02</u>	<u>0.11</u>	<u>-0.07</u>	<u>-0.57</u>	<u>-0.62</u>	<u>-0.43</u>	<u>-0.22</u>	/
<u>$\sigma_{\text{LW-WV}}$</u>	<u>2.27</u>	<u>3.45</u>	<u>3.53</u>	<u>3.11</u>	<u>2.84</u>	<u>2.57</u>	<u>2.72</u>	<u>2.15</u>	<u>1.73</u>	<u>1.77</u>	<u>2.31</u>	<u>2.89</u>	<u>3.54</u>
<u>$r_{\text{LW-WV}}$</u>	<u>-0.56</u>	<u>-0.45</u>	<u>-0.43</u>	<u>-0.50</u>	<u>-0.58</u>	<u>-0.57</u>	<u>-0.46</u>	<u>-0.13</u>	<u>0.38</u>	<u>0.13</u>	<u>-0.36</u>	<u>-0.58</u>	<u>-0.49</u>

600

	Annual 1	Jan	Feb	Mar	Apr	May	Jun	Jul	Aug	Sep	Oct	Nov	Dec
$\sigma_{SW-cloud}$	4.8676 1	0.01	0.16	1.201 1	4.5638 6	6.8459 7	12.5311 1	19.1461	14.4513 8	4.1632 1	0.6550	0.04	0
$r_{SW-cloud}$	0.3118	0.1514	0.272 2	0.413 6	0.4236	0.2916	0.1901	0.2105	0.3524	0.4026	0.3725	0.32	1
$\sigma_{LW-cloud}$	8.2502 3	8.8991 3	9.192 9	8.132 5	7.9664	10.7320	11.8191	14.0615 1	13.5556	13.6411 9	11.3110 0	10.311 8	9.838 6
$r_{LW-cloud}$	— 0.5246	— 0.5859	— 0.595 6	— 0.585 6	— 0.5551	— 0.4536	-0.0906	-0.0704	-0.3323	-0.6254	-0.5241	— 0.6460	— 0.585 6
σ_{SW-WV}	0.2729	0.001	0.03	0.14	0.3840	0.5759	0.7985	0.7785	0.5663	0.2833	0.0809	0.01	0
r_{SW-WV}	— 0.0702	— 0.0805	- 0.030 2	0.010 6	-0.0105	-0.0602	0.0611	-0.0807	-0.4957	-0.5662	-0.4443	— 0.2422	1
σ_{LW-WV}	2.2327	3.4045	3.465 3	3.071 1	2.8084	2.5157	2.5372	1.9221 5	1.5573	1.5877	2.2131	2.9689	3.615 4
r_{LW-WV}	— 0.6256	— 0.5045	— 0.484 3	— 0.565 0	— 0.6258	— 0.6057	-0.4846	-0.1213	0.3338	-0.0613	-0.5236	— 0.6758	— 0.574 9

605

610

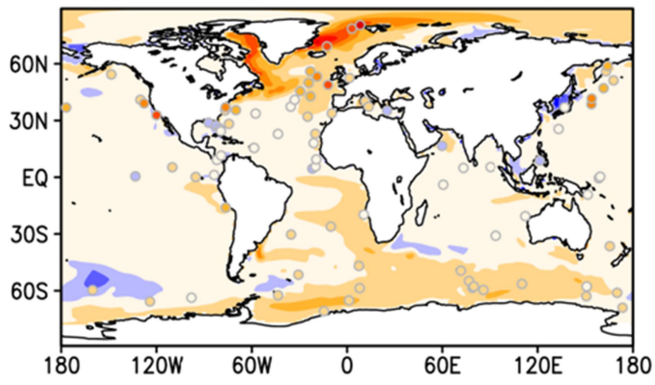
Table 3. The spatial standard deviation of sensible and latent heat flux anomalies σ_{SH} , σ_{LH} (Wm^{-2}) over the Arctic Ocean. r_{SH} and r_{LH} are correlation coefficients between SIC and sensible and latent heat flux anomalies, respectively. Those significant at a 99% confidence level are bolded.

	Jan	Feb	Mar	Apr	May	Jun	Jul	Aug	Sep	Oct	Nov	Dec
σ_{SH}	28.53	29.44	21.64	12.87	7.94	9.46	9.55	2.63	2.11	7.02	31.11	26.80
r_{SH}	0.57	0.64	0.67	0.66	0.76	0.26	<u>-0.36</u>	0.03	0.65	0.80	0.71	0.56
σ_{LH}	18.70	19.00	14.75	9.46	5.64	5.84	8.75	1.93	1.69	5.77	19.87	17.44
r_{LH}	0.74	0.77	0.78	0.76	0.71	0.14	<u>-0.42</u>	<u>-0.37</u>	0.69	0.90	0.79	0.72

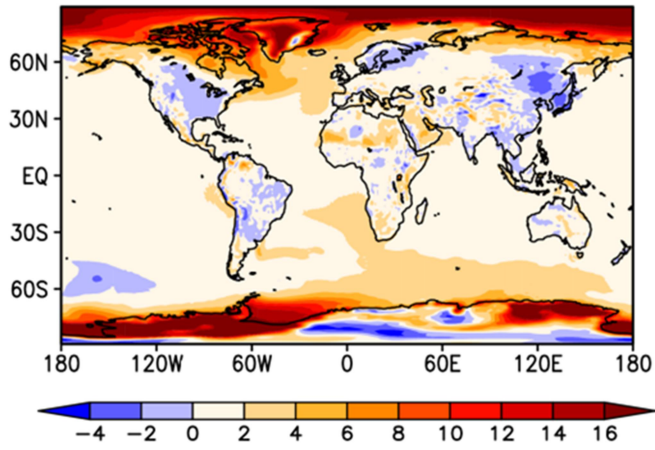
Table 4. The response coefficients (Wm^{-2}) of radiation and turbulent heat fluxes to the albedo and insulation effects of sea ice. Those significant at a 99% confidence level are bolded.

λ (Wm^{-2})	flux	Ann	Jan	Feb	Mar	Apr	May	Jun	Jul	Aug	Sep	Oct	Nov	Dec
albedo	SW	-	-	-	-	-	-	-	-	-	-	-	-	-
		<u>46.5</u>	0.0	<u>1.71</u>	<u>18.9</u>	<u>87.2</u>	<u>188.1</u>	<u>186.0</u>	<u>109.7</u>	<u>-77.5</u>	<u>34.4</u>	<u>4.75</u>	<u>-0.1</u>	0
		43.0			13.8	75.0	169.2	178.3	97.0	52.0	20.2			
	cloud	<u>4.32</u>	0.0	0.1	<u>1.10</u>	<u>4.43</u>	<u>4.62</u>	<u>6.10</u>	<u>11.3</u>	<u>13.79</u>	<u>4.23</u>	<u>0.64</u>	0.0	0
	SW													
insulation	WV	<u>-0.10</u>	0.0	0.0	0.0	0.0	<u>-0.10</u>	<u>0.12</u>	<u>-0.2</u>	<u>-1.07</u>	<u>0.45</u>	<u>-0.1</u>	0.0	0
	cloud	-	-	-	-	-	-	-	-	-	-	-	-	-
		<u>12.6</u>	<u>11.9</u>	<u>12.2</u>	<u>10.84</u>	<u>10.0</u>	<u>-11.4</u>	<u>-21.7</u>	<u>-</u>	<u>-12.2</u>	<u>21.3</u>	<u>15.2</u>	<u>16.4</u>	<u>-</u>
	LW	11.1	12.1	11.7		8.9	8.6		2.81	9.0	17.6	11.6	15.8	13.60
	WV	<u>-4.0</u>	<u>-</u>	<u>-</u>	<u>-3.95</u>	<u>-4.0</u>	<u>-3.64</u>	<u>-3.12</u>	<u>-0.79</u>	<u>1.49</u>	<u>-0.36</u>	<u>-</u>	<u>-5.0</u>	<u>-</u>
		3.9	3.95	3.84		3.7					2.30	4.4	4.81	
	SH	35.3	53.4	59.0	46.4	29.6	24.2	10.4	<u>-13.8</u>	0.4	7.1	22.3	79.2	54.0
	LH	27.7	45.3	46.0	36.6	25.0	16.1	3.5	<u>-15.0</u>	<u>-3.6</u>	6.0	20.5	56.7	45.7

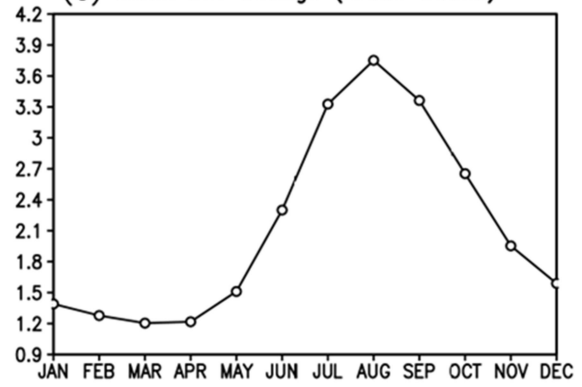
(a) SST change (Pliocene–Preindustrial)



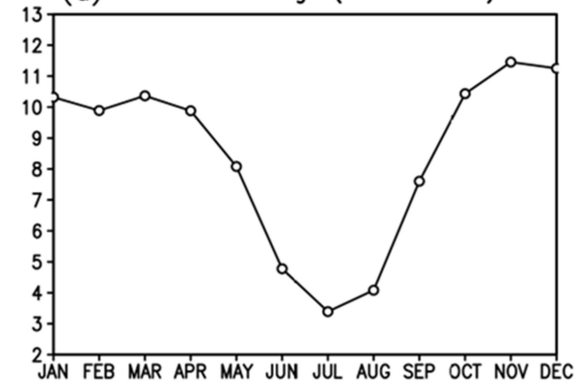
(b) SAT change (Pliocene–Preindustrial)

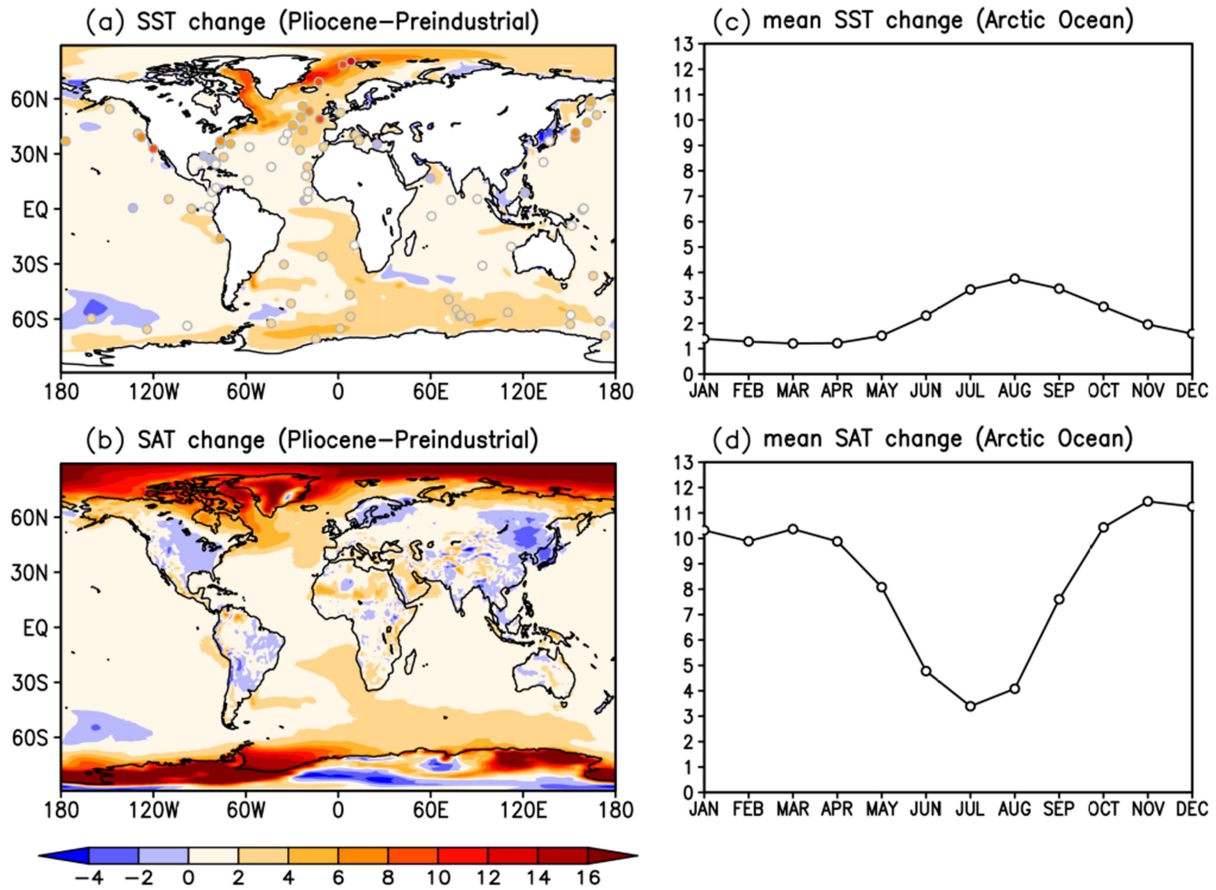


(c) mean SST change (Arctic Ocean)

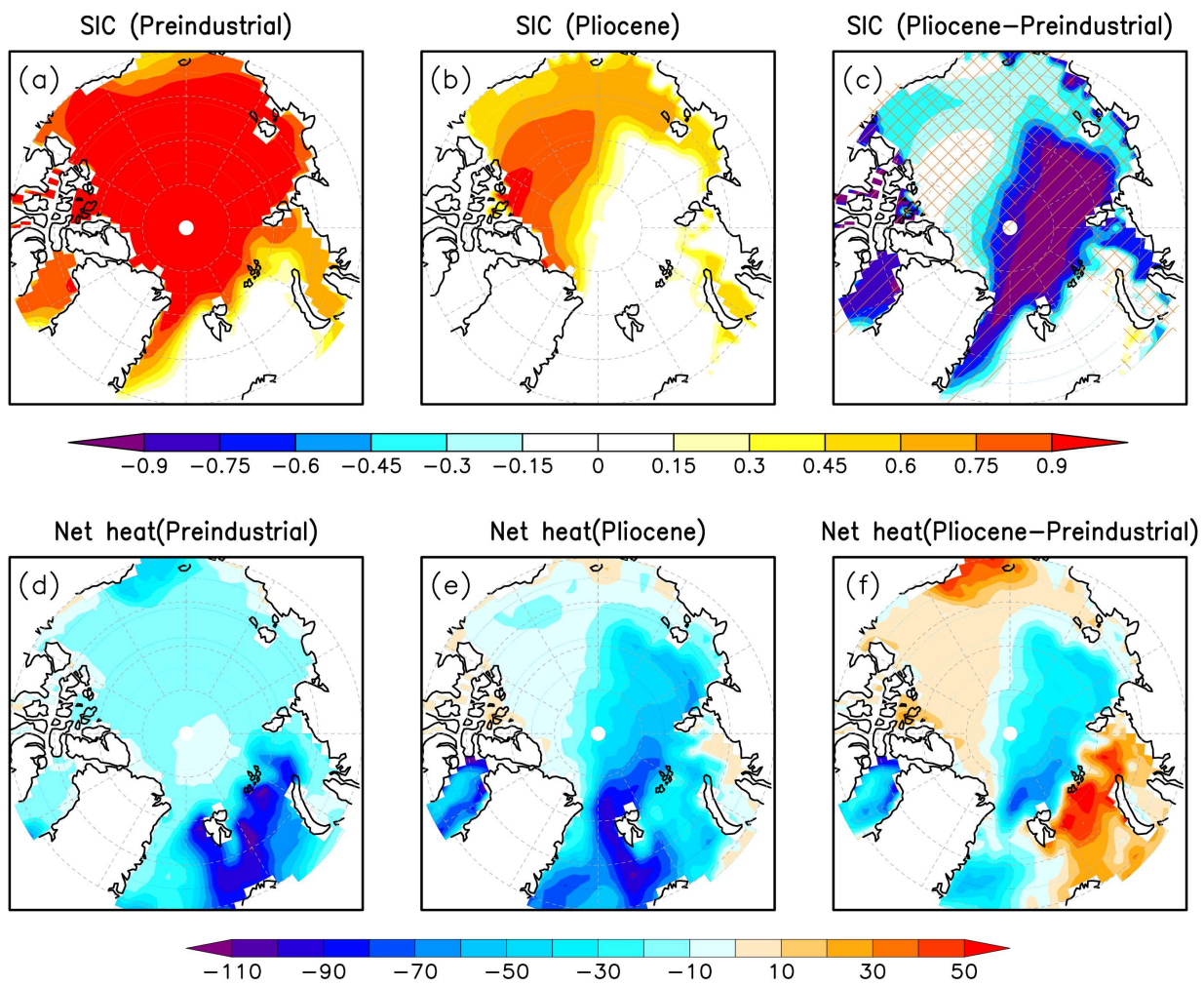


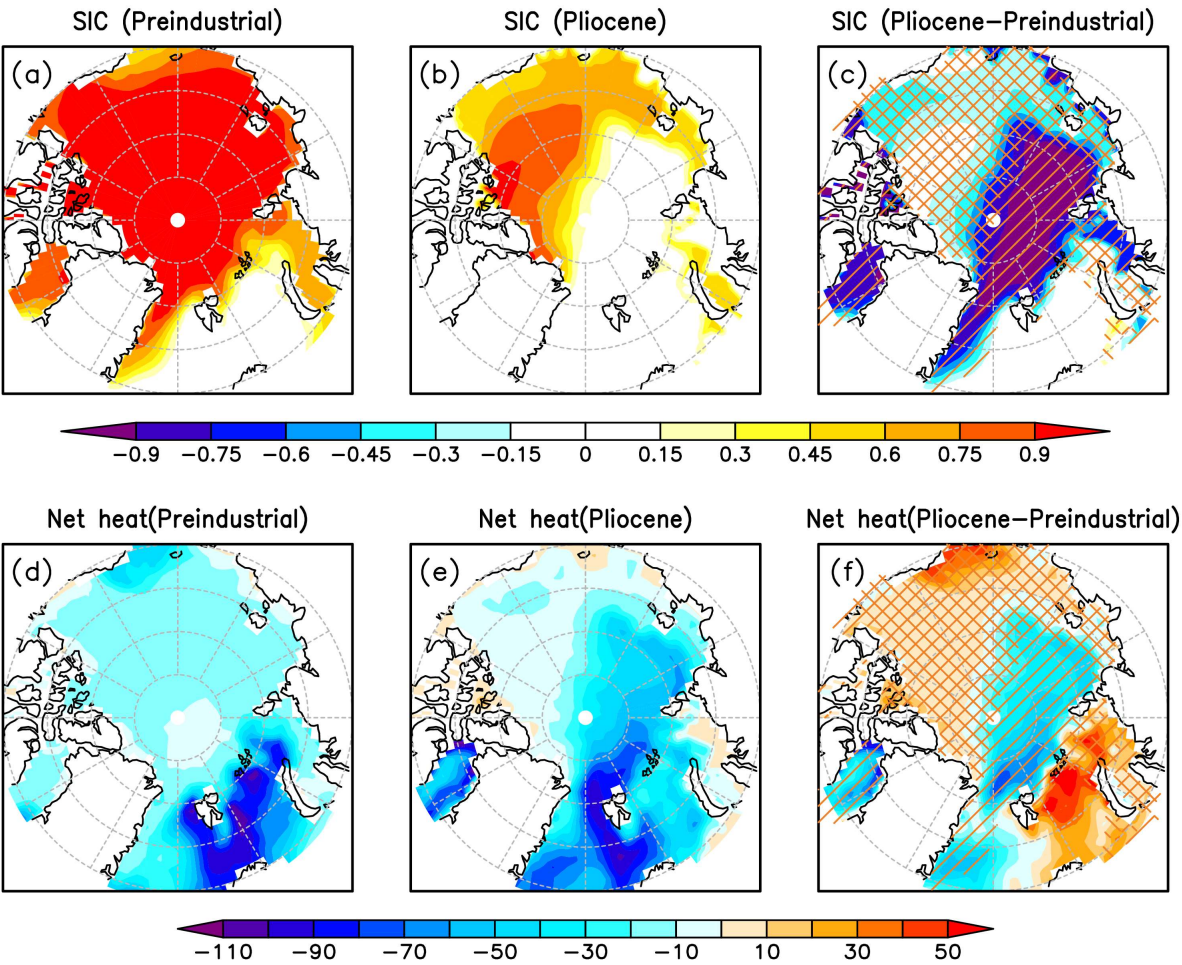
(d) mean SAT change (Arctic Ocean)





625 **Figure 1.** The annual mean warming (K) for (a) sea surface temperature (SST) and (b) surface air temperature (SAT), and seasonal warming (K) averaged over the Arctic Ocean for (c) SST and (d) SAT between the Pliocene and preindustrial simulations. The shaded circles in (a) represent the annual mean SST anomalies at 95% confidence-assessed marine sites from the Deep Sea Drilling Project (DSDP) and Ocean Drilling Program (ODP).

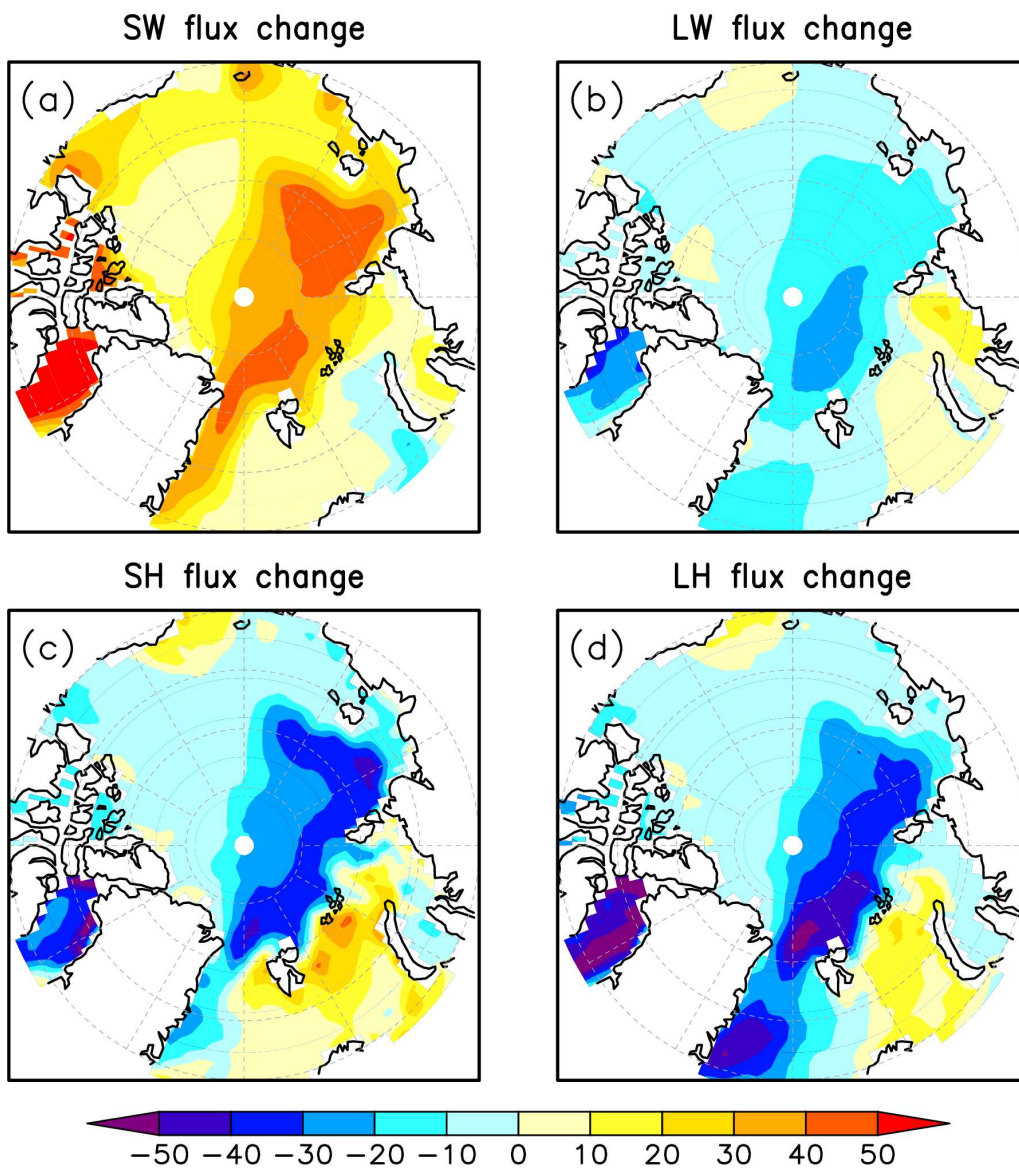




635

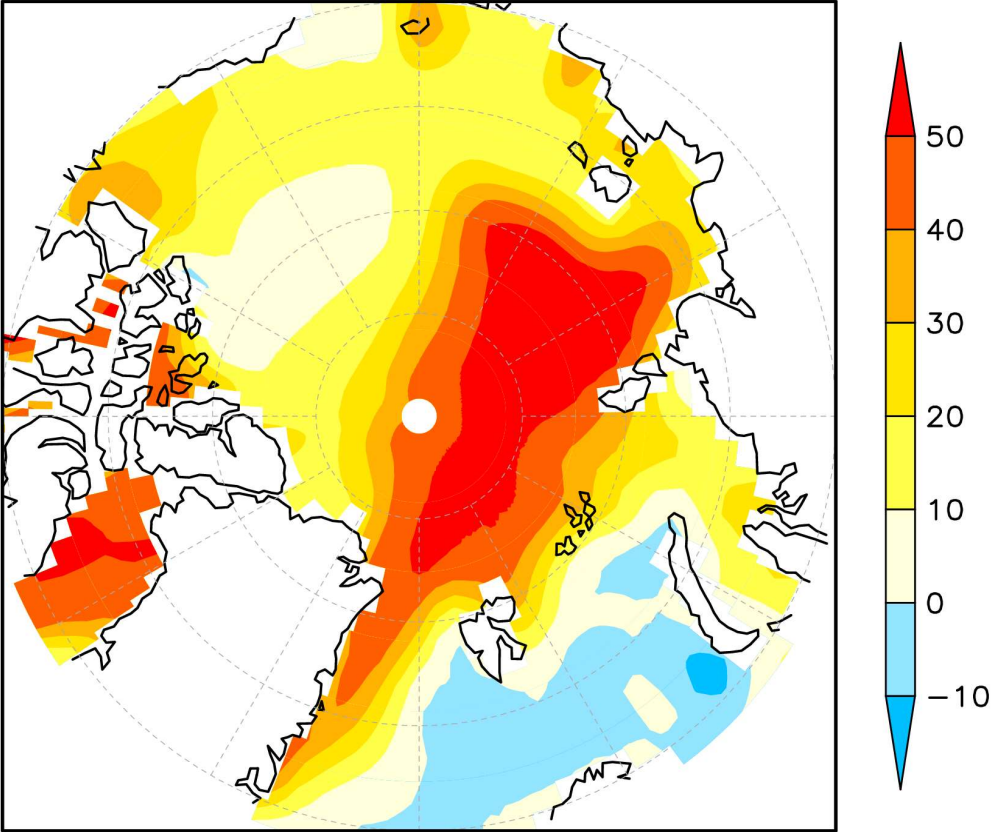
Figure 2. Spatial distributions of the annual mean sea -ice concentration (SIC) and ~~air-sea interface~~ net heat flux at the surface of ice and ocean (Wm^{-2} , positive downward) over the Arctic Ocean. (a) SIC in the preindustrial period, (b) SIC in the Pliocene, (c) the Pliocene SIC change with respect to the preindustrial period, (d) net heat flux in the preindustrial period, (e) net heat flux in the Pliocene, and (f) the Pliocene net heat flux change with respect to the preindustrial period. The diagonal stripe in (c) represents the regions from ice-covered to ice-free, and the diagonal crosshatch represents the regions from ice-covered to ice-covered.

640

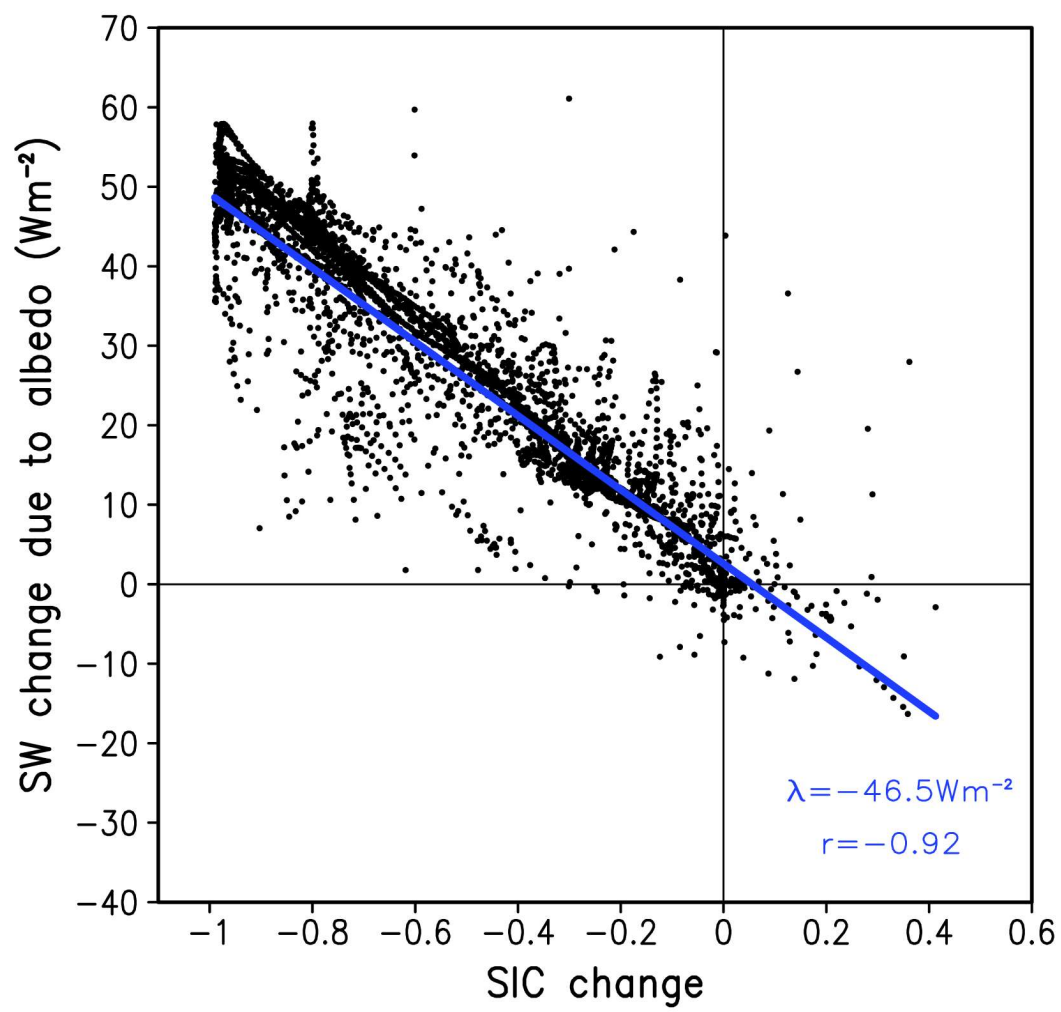


645 | **Figure 3.** Spatial distributions of the Pliocene annual mean heat flux change (Wm^{-2} , positive downward) with respect to the preindustrial period over the Arctic Ocean. (a) net shortwave radiation-flux, (b) net longwave radiation flux, (c) sensible heat flux, and (d) latent heat flux.

Mean annual SW change due to albedo effect



655 | **Figure 4.** Spatial distributions of the Pliocene annual mean net shortwave radiation-flux change (Wm^{-2} , positive downward) at the surface over the Arctic Ocean caused by albedo effect of sea -ice change with respect to the preindustrial period.



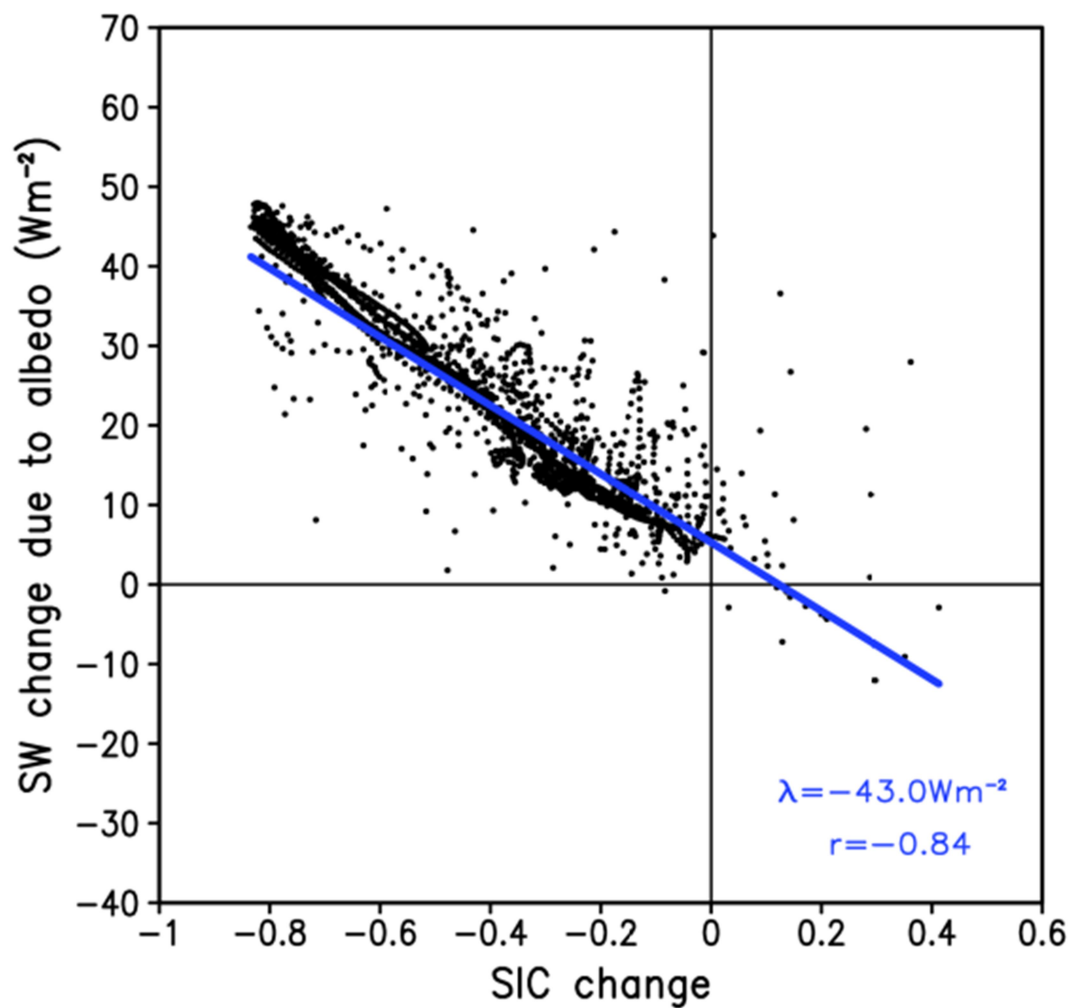
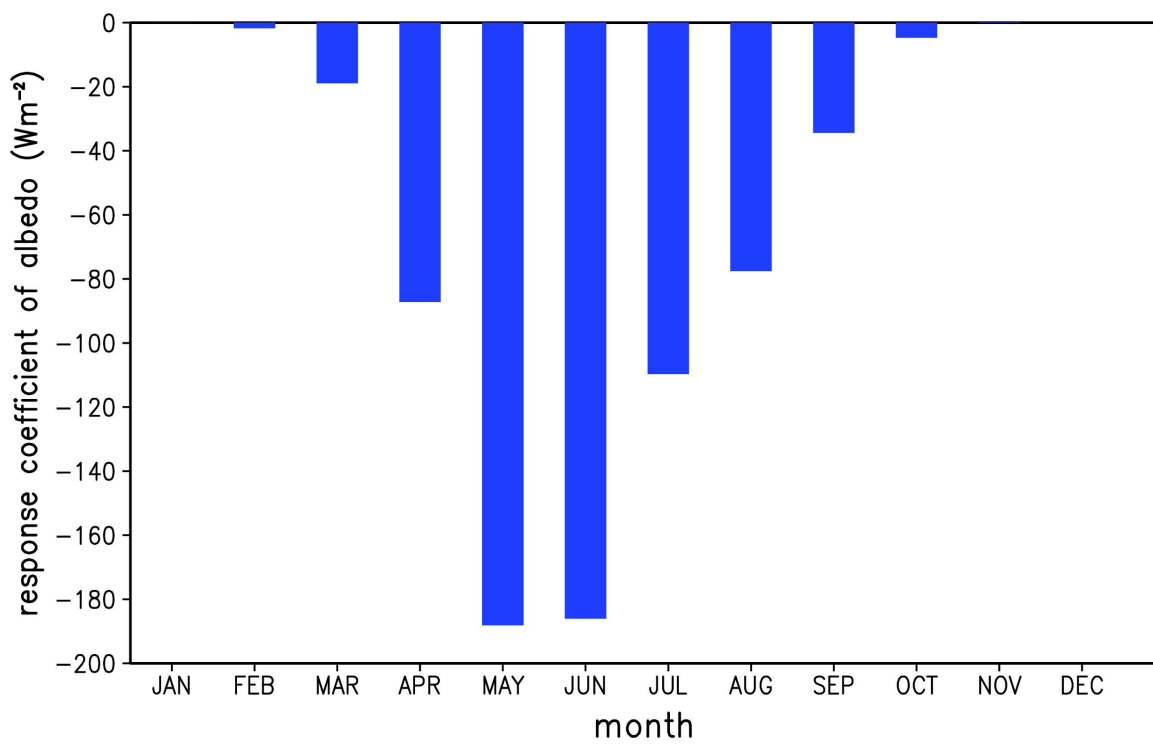
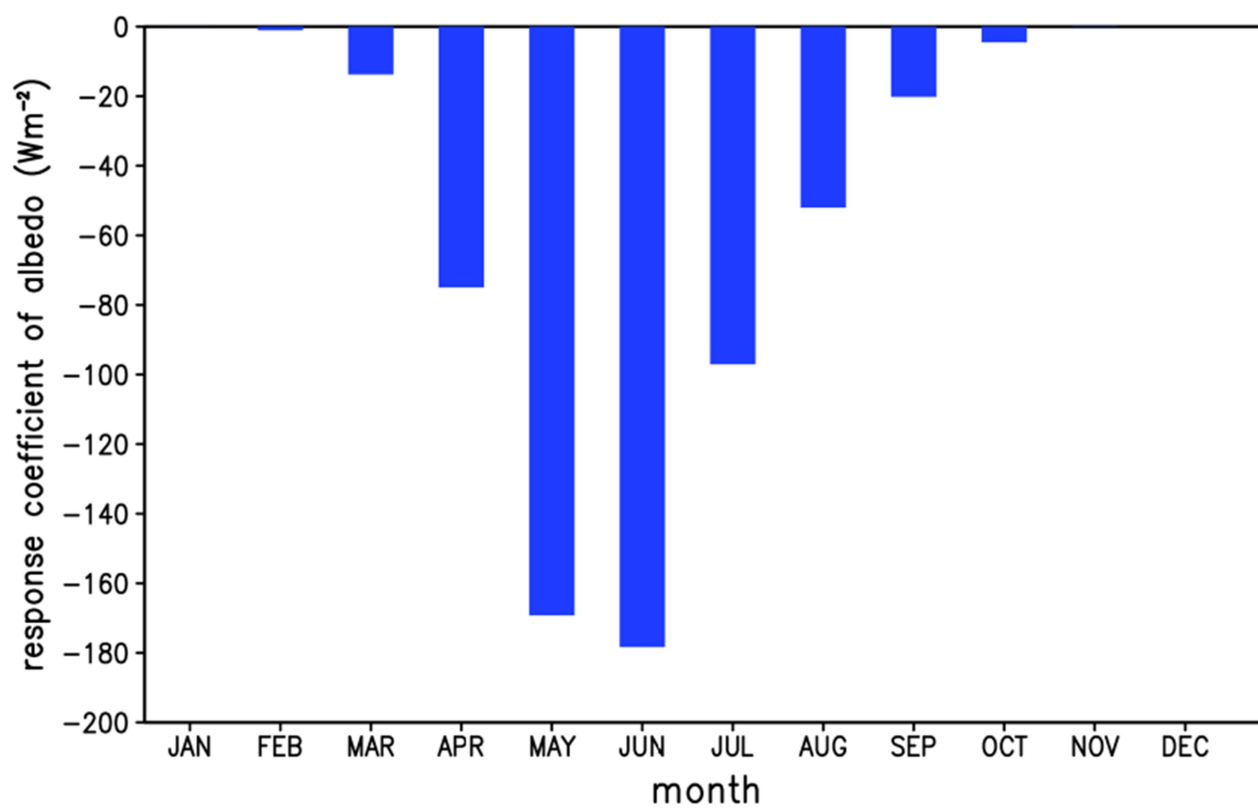


Figure 5. The annual mean net shortwave radiation-flux change (Wm^{-2} , positive downward) caused by the albedo effect of sea -ice change averaged over the Arctic Ocean as a function of SIC change. All the change areis with respect to the preindustrial period, and each dot represents one grid point value over the Arctic Ocean.





675 **Figure 6.** The monthly response coefficients (Wm^{-2}) of net shortwave ~~radiation~~-flux to the albedo effect of sea -ice.

680

685

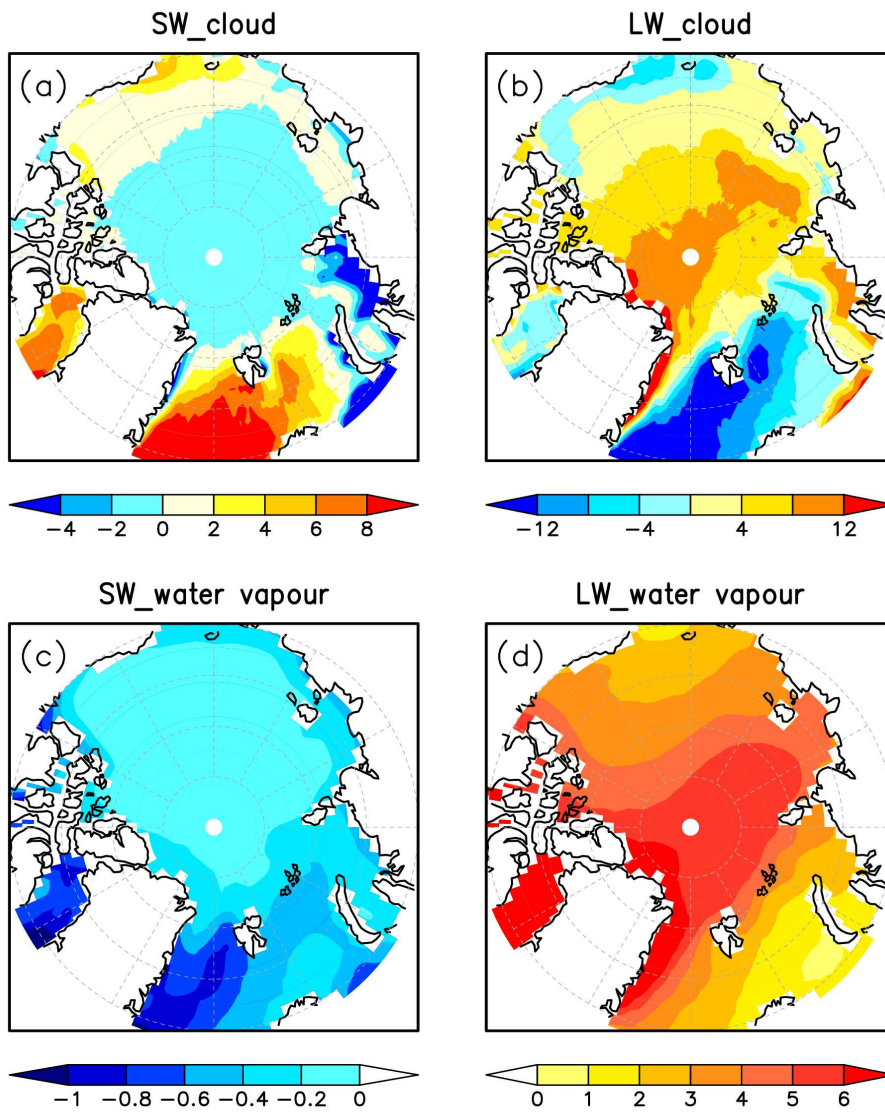
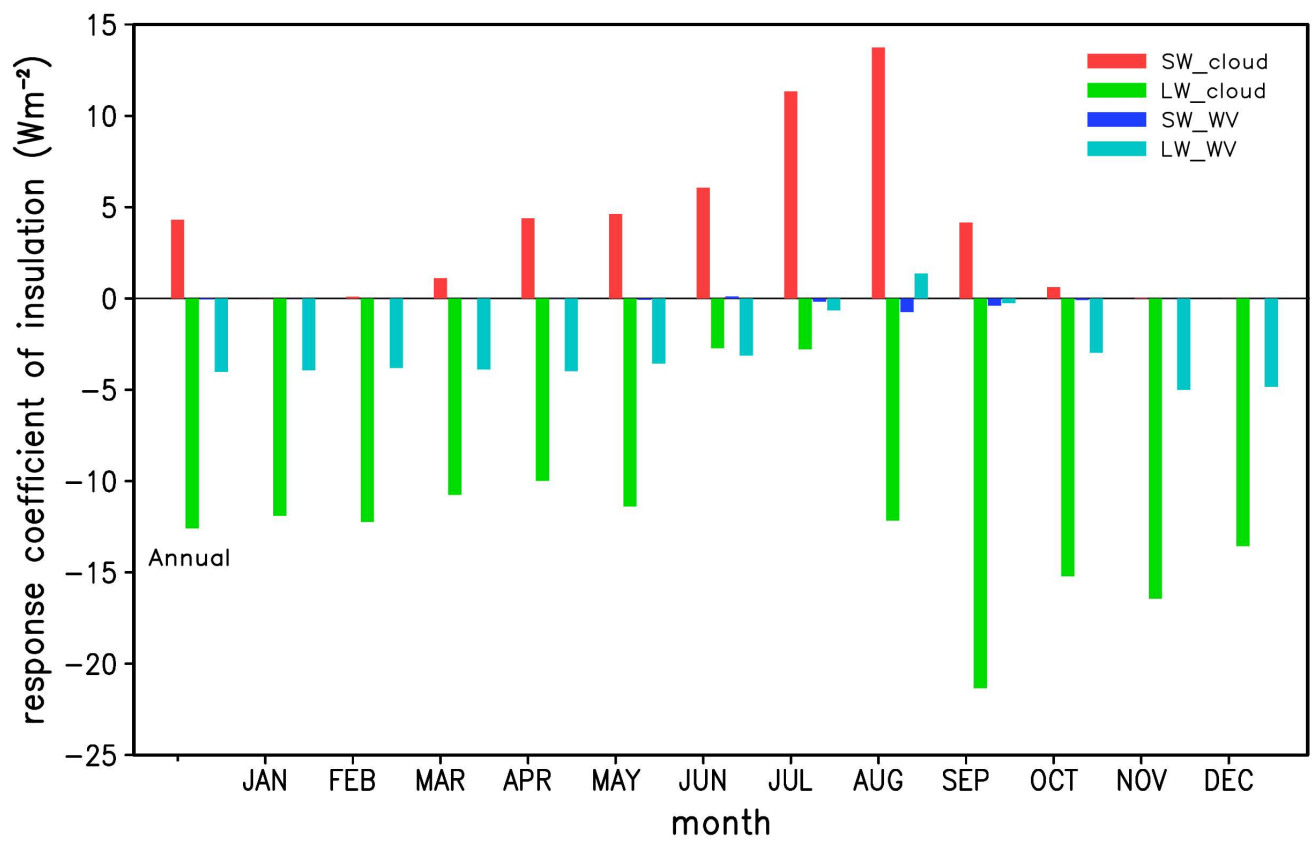


Figure 7. Spatial distributions of the Pliocene annual mean radiation fluxes change (Wm^{-2} , positive downward) with respect to the preindustrial period over the Arctic Ocean. (a) shortwave radiation due to cloud change, (b) longwave radiation due to cloud change, (c) shortwave radiation due to water vapour change, (d) longwave radiation due to water vapour change. Here ~~the~~₋ cloud and water vapour change is specified as the value before removing the part caused by sea-ice decrease remote effects of clouds and water vapour.



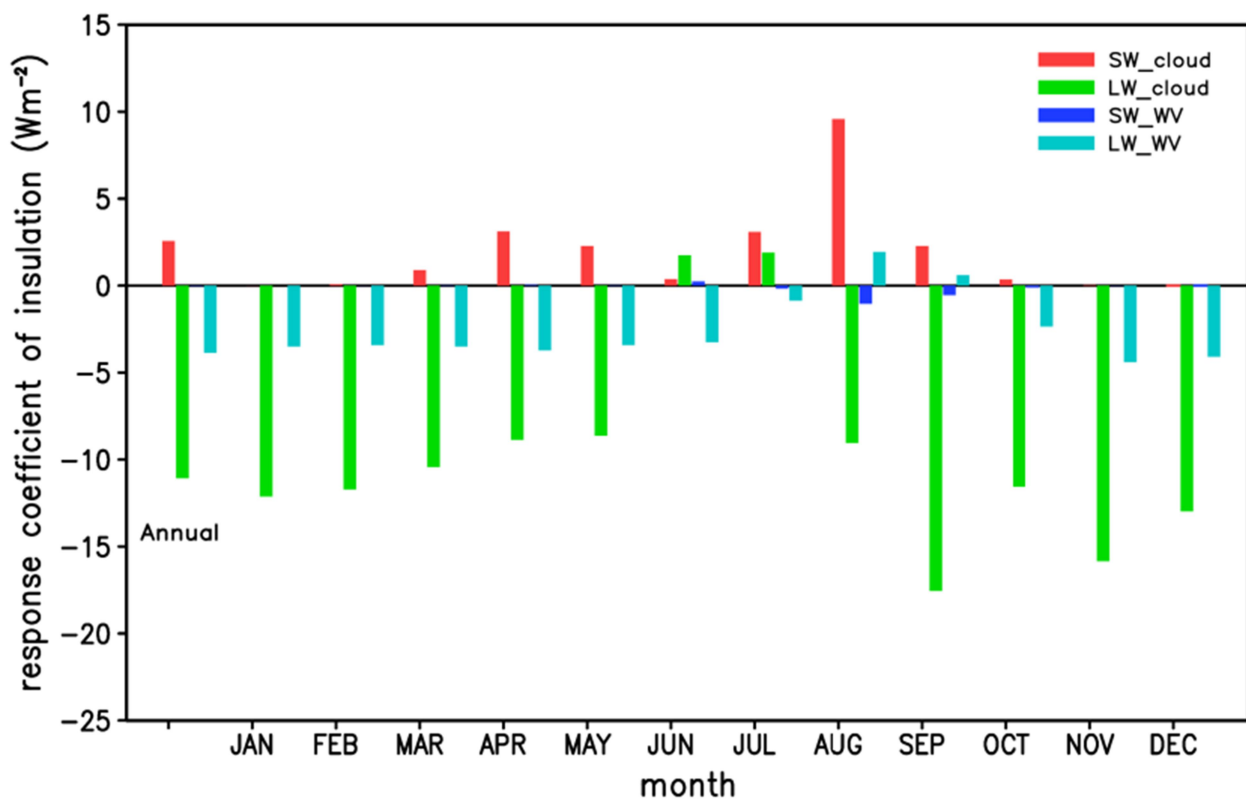


Figure 8. The annual and monthly response coefficients (Wm^{-2}) of net shortwave and longwave radiation flux ~~caused by~~related to cloud and water vapour change to the insulation effect of sea ~~ice~~. Here, the cloud and water vapour change is specified as the part ~~caused by~~related to sea ~~ice~~ decrease.

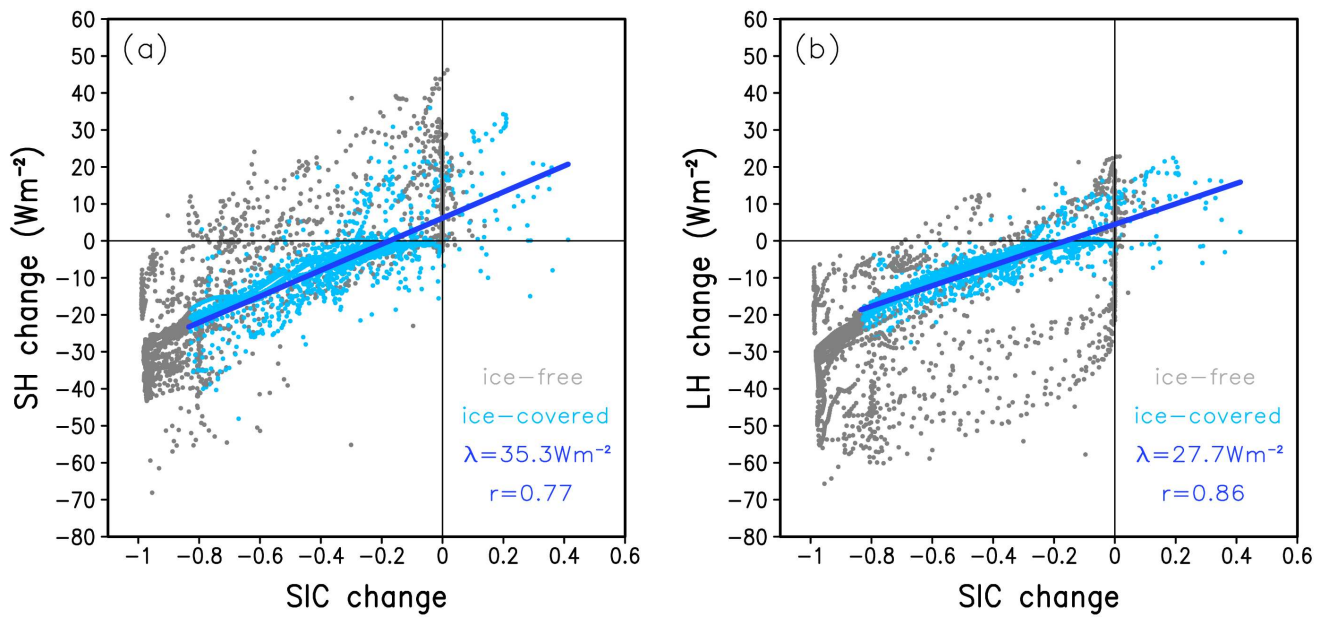
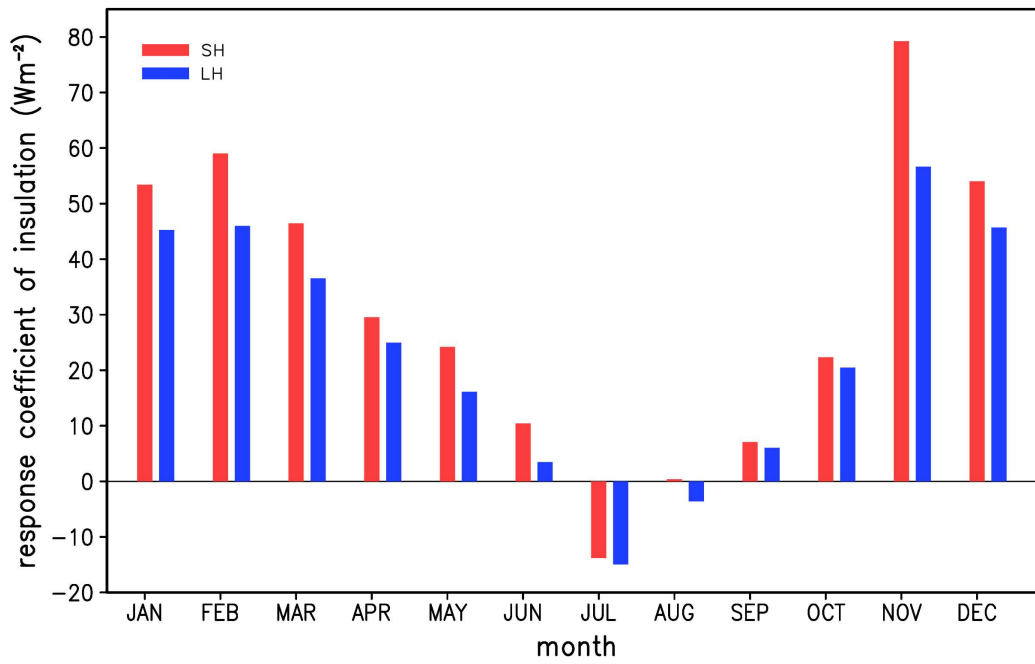


Figure 9. The annual mean sensible and latent heat flux change (Wm^{-2} , positive downward) caused by related to insulation effect of sea - ice change averaged over the Arctic Ocean as a function of SIC change. All the change Pliocene changes shown are with respect computed relative to the preindustrial simulation. The ice-free and ice-covered regions here refer to the diagonal hatched and cross-hatched regions in Figure 2c, respectively. The blue line is the linear regression on the ice-covered scatter points, and the response coefficient (λ) and correlation coefficient (r) are just for the ice-covered areas.



725 | **Figure 10.** The monthly response coefficients (Wm^{-2}) of sensible and latent heat fluxes to the insulation effect of sea ice.

Supplementary Information

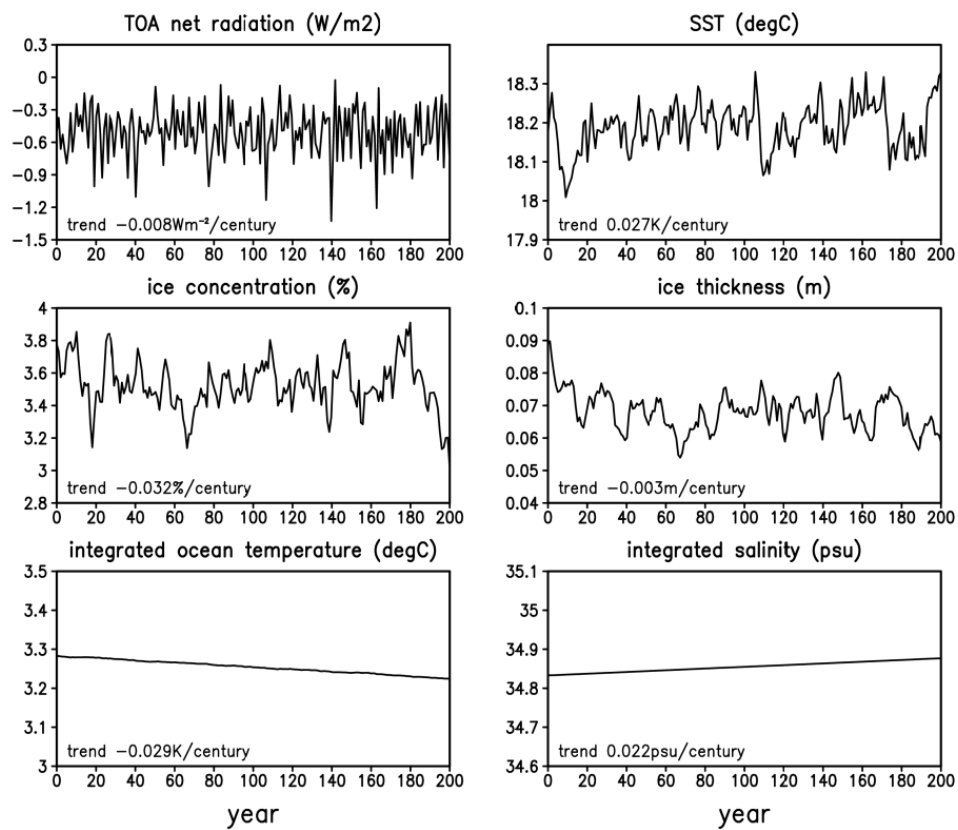


Figure S1. The global annual mean of last 200 model years output in the Pliocene simulation (The negative TOA net radiation represents a heat loss of the earth-atmosphere system.)

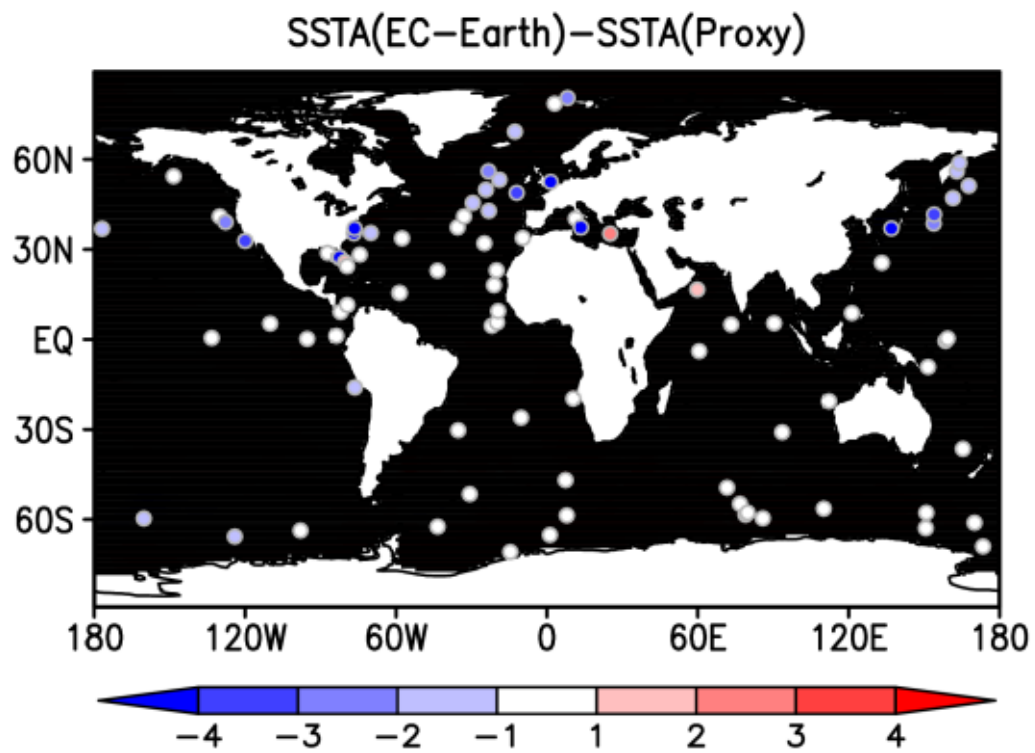


Figure S2. The difference of annual mean SST anomaly (Pliocene minus preindustrial, K) between EC-Earth simulation and the proxy data at 95% confidence-assessed marine sites from Deep Sea Drilling Project (DSDP) and Ocean Drilling Program (ODP).

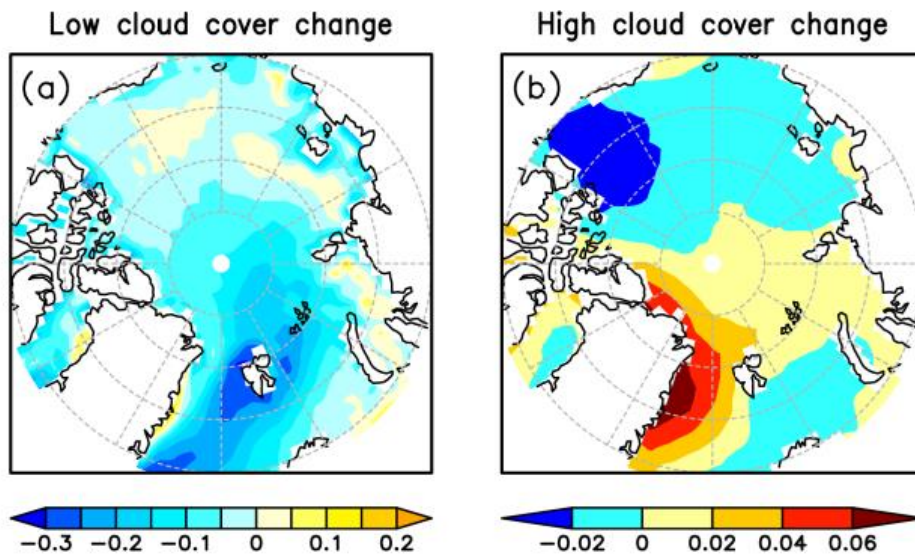


Figure S3. The difference of annual mean low cloud cover (a) and high cloud cover (b) anomaly in Pliocene with respect to the preindustrial.